

2018 Northeastern Veterinary Pathology Conference

NEVPC CASE 1

IDENTIFICATION NUMBER ON SOURCE MATERIAL: 4106953-00

CONTRIBUTOR: Erin E. Ball, DVM, DACVP

INSTITUTION: DOD Veterinary Pathology Residency Program, Joint Pathology Center, Silver Spring, MD

SIGNALMENT: 10-year-old castrated male Belgian malinois military working dog

HISTORY/PHYSICAL EXAM: This dog presented for acute onset bloody diarrhea and vomiting. On physical exam, he was weak and lethargic with dull mentation, tachycardia, tachypnea, and weak pulses. Thoracic and abdominal radiographs and ultrasound revealed free abdominal fluid and bilateral pleural effusion with lung compression. No thoracic or abdominal masses were noted. 1.3L of bloody fluid (which did not clot) was obtained via thoracocentesis; the total protein was 1.8g/dL and the PCV was 4.5%. Abdominocentesis revealed serosanguinous fluid with a total protein of 2.8 and a PCV of <1%. The pleural/peritoneal fluid was diagnosed as a transudate; cytologic evaluation (performed in-house) was suggestive of a neoplastic process. A chest tube was placed. Bloodwork revealed an elevated PCV (64%); mildly increased PT and aPTT; moderate leukocytosis with neutrophilia; severe hyperlactatemia; hyponatremia, hypochloremia, hyperphosphatemia, hyperkalemia, hypocalcemia, and mildly elevated ALT and AST. The patient continued to deteriorate, so humane euthanasia was elected and a necropsy was performed. This dog was treated for dirofilariasis in 2010.

GROSS FINDINGS: Severe thickening of the pericardium & epicardium (no culture performed due to lack of funds); bicavitary effusion (transudate); hemorrhagic lymphadenopathy (perihilar and tracheobronchial nodes); multiple "gritty" pulmonary nodules; hepatomegaly; gastric (pyloric) ulcers; and hemorrhagic enteritis

Careful examination and sectioning failed to reveal a solid neoplasm.

CYTOLOGIC FINDINGS: Pleural fluid (not submitted): Aspirates are composed of individualized and clustered round to polygonal cells admixed with mildly increased numbers of neutrophils, foamy macrophages, and small lymphocytes. Polygonal cells are characterized by a moderate amount of dark blue cytoplasm and an oval nucleus, with coarse chromatin and occasionally prominent nucleoli. Cells are often encircled by an eosinophilic to basophilic coronal "fringe." Anisocytosis and anisokaryosis are moderate to marked, and there are frequent binucleate and multinucleate cells. Mitoses are not observed.

CYTOLOGIC IMPRESSION: Pleural fluid: Mesothelial reactive hyperplasia or neoplasia.

HISTOPATHOLOGIC FINDINGS:

Pericardium: The pericardium is thickened up to 6mm by dense fibrous connective tissue with abundant hemorrhage and scattered hemosiderin laden macrophages. Multifocally, pericardial

lymphatics and vessels contain clusters of round to polygonal cells with a moderate amount of eosinophilic cytoplasm and an oval nucleus, with dense chromatin and indistinct nucleoli. Mitoses are not seen. These cells are consistent with mesothelial cells. Several sections (not submitted) of pericardium, epicardium, pleura and aortic adventitia exhibit moderate to severe mesothelial hyperplasia, with multifocal formation of papillary projections.

Tracheobronchial lymph node: The subcapsular and medullary sinuses are markedly expanded by individual and clustered round to polygonal cells with a moderate amount of eosinophilic cytoplasm and an oval nucleus with dense chromatin and indistinct nucleoli. Anisocytosis and anisokaryosis are moderate. There are frequent bi- and multinucleate cells. These cells (consistent with mesothelial cells) often contain a discrete vacuole that peripheralizes the nucleus. There is also draining hemorrhage and hemosiderosis.

Immunohistochemistry: Round to polygonal cells within the lymph node sinuses exhibit diffuse, strong cytoplasmic immunoreactivity to pan-cytokeratin. Vimentin, WT-1 and TTF-1 are negative. Calretinin is non-contributory.

The liver (not submitted) exhibits evidence of chronic-passive congestion with dilated/congested sinuses, moderate to severe edema, centrilobular fibrosis, and scattered foci of hemosiderin-laden macrophages.

Within the lung (not submitted), multiple pulmonary arteries are variably occluded by marked granulomatous and proliferative arteritis with mineralized thrombi and adult nematodes consistent with *Dirofilaria immitis*.

MORPHOLOGIC/ETIOLOGIC DIAGNOSIS:

1. Pericardium: Fibrosis, diffuse, severe, with multifocal hemorrhage, hemosiderosis, and mesothelial hyperplasia.
2. Tracheobronchial lymph nodes; pericardial lymphatics: Embolized mesothelial cells.
3. Liver (not submitted): Congestion, chronic, diffuse, severe with centrilobular fibrosis, edema, and hemosiderosis.
4. Lung, pulmonary arteries (not submitted): Arteritis, granulomatous and proliferative, multifocal, severe, with mineralized thrombi and adult *Dirofilaria immitis*.

DISCUSSION: The histologic features in the pericardium and epicardium, in combination with the reported physical exam and gross necropsy findings, are consistent with constrictive pericarditis. This likely led to chronic cardiac compression, impaired diastolic filling, venous engorgement with diminished cardiac output, and right sided (+/- left sided) heart failure, with subsequent pleural effusion, ascites and chronic-passive hepatic congestion. We hypothesize that pleural effusion resulted in mesothelial hyperplasia with embolization of mesothelial cells to regional lymph nodes. The cells in question are cytokeratin positive, but vimentin negative, which does not rule out metastatic carcinoma cells (versus mesothelium); however, based on the morphologic features, the lack of any solid tumor, and the presence of pleural effusion and mesothelial hyperplasia, we favor a diagnosis of reactive mesothelial hyperplasia with mesothelial emboli.

Reactive mesothelial hyperplasia is a well-documented lesion associated with pleural effusion, while embolization of benign mesothelial cells to regional lymph nodes is rarely reported in humans and animals. All reported cases have been associated with pleural/peritoneal effusions or pericarditis, as in this case. The proposed pathogenesis of multicentric embolic reactive mesothelium (MERM) involves desquamation of hyperplastic mesothelial cells into an effusion, with subsequent clearance through intercellular mesothelial stomata (which connect with submesothelial lymphatics), and accumulation in draining lymph nodes. It can be very difficult to distinguish MERM from metastatic mesothelioma or carcinoma, as reactive mesothelium often exhibits features of malignancy. Lack of a solid tumor, as well as a histologic lack of papillary formations, stromal reaction, or invasiveness within the lymph node, are all suggestive of MERM (rather than neoplasia).

The most common causes of constrictive pericarditis in humans (and likely domestic animals as well) are infectious (bacterial, viral or fungal) or idiopathic, though neoplasia, trauma and various other etiologies are reported. Typical clinical findings include tachycardia, dyspnea, ascites, pleural effusion, pericardial effusion, hepatosplenomegaly. The underlying cause of the pericardial fibrosis in this case is unclear. A culture was not performed, so we cannot rule out an infectious etiology. Though there is no histologic evidence of active infection, it is possible that the lesions represent the late stage/reparative phase of a chronic infection. Canine idiopathic hemorrhagic pericardial effusion (IHPE), a disease characterized by accumulation of serosanguineous pericardial fluid without evidence of any underlying disorder, was also suggested as a possible cause. IHPE has been associated with pericardial thickening and fibrosis; however, it tends to be slowly progressive in nature. In this case there is no history of clinical signs attributable to pericardial effusion and the presence of pericardial effusion was not noted grossly during the necropsy.

In light of the presence of pulmonary proliferative arteritis with mineralized thrombi and adult nematodes, we also wondered whether the previous heartworm disease could have played a role in this dog's clinical presentation. While pulmonary arteritis with subsequent chronic pulmonary hypertension, right-heart failure, ascites, chronic-passive hepatic congestion and pleural effusion are well-documented sequelae to canine dirofilariasis, we are unaware of any reported cases of fulminant constrictive pericarditis secondary to heartworm disease in dogs.

In conclusion, this report describes a case of embolization of benign, reactive mesothelial cells to regional lymph nodes in a dog with constrictive pericarditis and pleural effusion, a lesion which is rarely documented in domestic animals.

REFERENCES:

1. Caswell JL, Williams KJ. Respiratory system. In: Maxie MG, ed. *Jubb, Kennedy, and Palmer's Pathology of Domestic Animals*. Vol 2. 6th ed. St. Louis, MO: Elsevier Limited; 2016:520-523.
2. Dabbs DJ, ed. *Diagnostic Immunohistochemistry: Theranostic and Genomic Applications*. 4th ed. Philadelphia, PA: Elsevier Saunders; 2014: 474-478, 838).
3. Diaz-Delgado J, et al. Multicentric benign epithelial inclusions in a free-ranging Risso's dolphin (*Grampus griseus*). *J Comp Path*. 2016;155: 267-271.

4. Epstein SE. Exudative pleural diseases in small animals. *Vet Clin Small Anim.* 2014;44:161-181.
5. Goupil A, Bolliger C, Lapointe C, Morency A, Girard C. Embolised mesothelial cells in a tracheobronchial lymph node associated with idiopathic chylopericardium in a dog. *J Small Anim Pract.* 2012;53(11):664-667.
6. Little AA, Steffey M, Kraus MS. Marked pleural effusion causing right atrial collapse simulating cardiac tamponade in a dog. *J Am Anim Hosp Assoc.* 2007;43:157-162.
7. Machida N, et al. Development of pericardial mesothelioma in golden retrievers with a long-term history of idiopathic haemorrhagic pericardial effusion. *J Comp Path.* 2004;131, 166–175
8. Mehta A, Mehta M, Jain AC. Review: Constrictive pericarditis. *Clin Cardiol.* 1999;22:334-344.
9. Mellanby RJ, Villiers E, Herrtage ME. Canine pleural and mediastinal effusions: A retrospective study of 81 cases. *J Small Anim Pract.* 2002;43(10):447-451.
10. Padrid P. Canine and feline pleural disease. *Vet Clin North Am Small Anim Pract.* 2000;30(6):1295-1307.
11. Parkash V, Vidwans M, Carter D. Benign mesothelial cells in mediastinal lymph nodes. *Am J Surg Pathol.* 1999;23(10):1264-9.
12. Peters M, Tenhundfel J, Stephan I, Hewicker-Trautwein M. Embolized mesothelial cells within mediastinal lymph nodes of three dogs with idiopathic hemorrhagic pericardial effusion. *J Comp Pathol.* 2003;128:107-112.
13. Pizzi M, et al. Benign mesothelial cells in lymph nodes and lymphatic spaces associated with ascites. *Histol Histopathol.* 2016; 31:747-750.
14. Robinson WF, Robinson NA. Cardiovascular system. In: Maxie MG, ed. *Jubb, Kennedy, and Palmer's Pathology of Domestic Animals.* Vol 3. 6th ed. St. Louis, MO: Elsevier Limited; 2016:24-26;83-85.
15. Valenciano AC, Arndt TP, Rizzi TE. Effusions: Abdominal, thoracic and pericardial. In: Valenciano AC, Cowell RL, eds. *Cowell and Tyler's Diagnostic Cytology and Hematology of the Dog and Cat.* 4th ed. St. Louis, MO: Elsevier Mosby; 2014: 247-248.

ACKNOWLEDGEMENTS:

- Dr. Bruce Williams, Joint Pathology Center
- MAJ Robert Kim, Joint Pathology Center
- Dr. Michael Lagutchik, DOD Military Working Dog Veterinary Service
- Special thanks to the WRNMMC laboratory for providing outstanding histology and immunohistochemical technical support

2018 Northeast Veterinary Pathology Conference – Gaithersburg, MD

April 7-8, 2018

Case Submission Form

NEVPC CASE #2

IDENTIFICATION NUMBER ON SOURCE MATERIAL: 210884-17 Cornell University

CONTRIBUTORS: W. Shane Sills, DVM; Katie Kelly, DVM, PhD, DACVP

INSTITUTIONS: Cornell University Department of Biomedical Sciences; Section of Anatomic Pathology

SIGNALMENT: 5-year old, male castrated, English Springer Spaniel dog

HISTORY:

A surgical biopsy of liver was received on December 17, 2017. Per the submitting veterinarian, this dog has a previous history of elevated copper (517 ppm), and has a previous cholecystectomy for treatment of a gallbladder mucocele. Previous biopsy, dated February 24, 2017 from a different pathology laboratory indicated cystic mucinous hyperplasia in the gallbladder and chronic hepatitis with eosinophils, neutrophils, and sub-bridging fibrosis, with a 3/5 copper accumulation using a copper-identifying histochemical stain.

GROSS FINDINGS:

Submitted to the Animal Health Diagnostic Center Section of Pathology, Cornell University, College of Veterinary Medicine was a single jar containing a 6.0 x 5.0 x 2.2 cm, formalin fixed, wedge section of liver. The liver is described in the clinical history as having a mottled appearance with rounded margins.

HISTOPATHOLOGIC FINDINGS:

Liver (Slides 1-3): Examined are sections of liver with similar histologic changes. Multiple central veins in different sections are occluded by variably organized coagula of fibrin with entrapped leukocytes, predominantly neutrophils (fibrin thrombi). Entrapped leukocytes within thrombi are generally viable, with only rare cells exhibiting degeneration characterized by condensation of nuclei and loss of

cytoplasmic detail. The lymphatics of central veins are diffusely dilated, and the adventitia is expanded by irregular bundles of collagen. In many areas, the central vein is obscured by the lymphatic dilation and fibroplasia, with dilation of adjacent sinusoids. The adventitia of portal tracts is expanded by irregular collagen, which frequently forms peripheral tendrils that stretch toward adjacent tracts (incomplete portal to portal bridging fibrosis). Occasionally, similar tendrils extend from the portal tracts to nearby central veins (incomplete portal to central bridging fibrosis). Diffusely, central veins are closely approximated to adjacent portal tracts (lobular atrophy). Portal tracts are often elongated and contain stout, thick arterioles. The hepatocytes diffusely contain variable amounts of clear, ill-defined, cytoplasmic vacuoles separated by thin wisps of cytoplasm (glycogen accumulation). Rare aggregates of lipofuscin-laden macrophages (lipogranulomas) infiltrate portal tracts.

The following histochemical staining was performed on the liver:

Reticulin (reticular matrix): Reticular fibers around many central veins are condensed and tightly layered (parenchymal collapse). In some areas, sinusoids around central veins are shrouded by cross-strutting fibers of the reticular substructure. The lobular atrophy is accentuated, and hepatocytes retain radial arrangement between central veins and portal tracts. The reticular matrix is obscured in some areas by severe glycogen accumulation.

Masson trichrome (collagen): Incomplete bridging fibrosis between portal tracts and occasional central veins is confirmed with light blue staining of collagen fibers extending from portal tract adventitia. In most areas, chicken-wire dissected fibrosis extends radially from central veins, tracking through sinusoids for at least 8-10 cells in length. Fibrin thrombi are accentuated by the counterstain but do not contain fibrillar collagen.

Prussian blue (iron): There is a minimal accumulation of iron in approximately 1/3 of Kupffer cells and in rare portal lipogranulomas.

Rhodanine (copper): Throughout the examined sections, up to 30% of centrilobular hepatocytes, and scattered periportal hepatocytes contain moderate amounts of copper. This corresponds to a grade 3/5, where grade 0 has no stainable copper and grade 5 has a panlobular accumulation of copper.

MORPHOLOGIC DIAGNOSES:

Liver:

1. Moderate, multifocal, sub-acute, central vein thrombosis with portal-to-portal and portal-to-central incomplete bridging fibrosis, centrilobular dissecting fibrosis, and centrilobular parenchymal collapse (Budd-Chiari-like Syndrome)
2. Moderate, generalized, hepatocellular copper accumulation (grade 3/5)
3. Moderate, diffuse, glycogen-type vacuolar hepatopathy
4. Portal vein hypoperfusion

DISCUSSION:

Histologic examination of several liver sections revealed numerous central vein fibrin thrombi with central vein remodeling characterized by increased collagen deposition in the adventitia, dilation of central vein lymphatics, dissecting fibrosis, and dilation of adjacent sinusoids. Chronic central vein remodeling in conjunction with numerous fibrin thrombi raise concern for hepatic venous outflow obstruction. This constellation of histologic changes is reflective of hepatic venous outflow obstruction, similar to the condition in humans termed 'Budd-Chiari Syndrome'.

In humans, hepatic venous outflow obstruction is classified into three distinct entities, depending on the level of the vascular tree that is affected. Obstruction at the level of the sinusoids or terminal venules is termed 'veno-occlusive disease'. Obstruction at the heart, as seen in right-sided congestive heart failure or cor pulmonale, is termed 'congestive hepatopathy'. Obstruction from the level of the superior end of the inferior vena cava to the hepatic veins, similar to our case, is termed 'Budd-Chiari Syndrome' (Bayraktar, et al 2007). Budd-Chiari Syndrome may be subdivided into primary disease, caused by primary venous disease, such as thrombosis, stenosis, or phlebitis, and secondary disease, caused by compression or obstruction by a lesion beyond the venous system (Plessier and Valla, 2008; Ferral et al 2012).

Budd-Chiari Syndrome (BCS) in humans is frequently associated with a hypercoagulable state, and is most commonly associated with myeloproliferative diseases that increase blood viscosity, such as polycythemia vera or essential thrombocytosis, as well as sickle cell anemia (Zimmerman, et al 2006). Different reports indicate myeloproliferative disease is associated with anywhere from 40-50% of BCS cases in humans (Patel, et al 2006; Plessier and Valla, 2008). Several hypercoagulable states, including inherited and acquired varieties, have been implicated in the development of BCS (Menon, et al 2004).

Budd-Chiari Syndrome develops as venous outflow of the hepatic veins is obstructed, which results in increased sinusoidal pressure, leading to chronic hypoxia, centrilobular hepatocyte loss, and fibrosis. In severe cases, remodeling will result in nodular regeneration and eventual cirrhosis. In chronic cases,

obstruction of outflow often results in portal vein hypertension and thrombosis, with development of acquired portosystemic shunts and ascites (Menon, et al 2004).

Clinically, human patients often present with elevated serum aspartate and alanine aminotransferases, and occasionally with serum alkaline phosphatase or bilirubin increases as well. Doppler ultrasonography is a powerful diagnostic tool, with a sensitivity and specificity of 70-85%, and computed tomography and magnetic resonance imaging are useful adjuncts for identifying hepatocellular necrosis, venous patency, and ascites (Menon, et al 2004; Zimmerman, et al 2006).

Budd-Chiari syndrome is a rare entity in veterinary medicine, and the term has previously been used to refer to any condition resulting in post-hepatic venous obstruction (Schoeman and Stidworthy 2001). In veterinary medicine, the term 'Budd-Chiari-like Syndrome (BCLS)' is preferred (Grooters and Smeak 1995). Like human BCS, canine BCLS may be associated with any prothrombotic condition, such as vasculitis, Cushing's syndrome, neoplasia, or infection. More specifically, vascular invasion by tumors, such as a pheochromocytoma, has been implicated in BCLS (Schoeman and Stidworthy 2001), as well as caval syndrome in dirofilariasis (Otto, et al 1990). Congenital obstruction of the inferior/caudal vena cava by a fibrinous web or diaphragm has been described in both humans and dogs (Otto, et al 1990; Ferral, et al 2012). Other congenital cardiac conditions, such as cor triatrium dexter, as well as cardiac neoplasms, have been associated with the development of BCLS in dogs (Otto, et al 1990; Gulcubuk, et al 2012).

The cause of thrombosis was not evident in this case. In this case, there is no histologic evidence of vasculitis, although vasculitis may be present elsewhere. Vasculitis is typically due to an infectious etiology, neoplasia, or drug reaction. Given the diffuse hepatocellular glycogen accumulation, it is possible this dog was hypercoagulable secondary to hyperadrenocorticism (Cushing's disease). In dogs, glycogen accumulation is attributable to excess glucocorticoids, either endogenous (e.g., Cushing's disease) or exogenous (e.g., iatrogenic) sources, in up to 50% of cases (Sepesy, et al 2006). The lobular atrophy in this case is attributed to portal vein hypoperfusion caused by chronic venous outflow obstruction, leading to centrilobular parenchymal collapse.

Histochemical stains also confirmed a significant copper accumulation. Copper-associated hepatopathy is a well-described, chronic inflammatory condition in dogs. Chronic excess accumulation of copper in the liver of dogs can be hereditary (e.g. Bedlington terrier) or acquired. Dogs can be exposed to copper sulfate in a wide range of household products (e.g. fungicides, algacides, and fertilizers). Copper ions can be released from copper water pipes in an acid pH. Some domestic water supplies are naturally high in copper. However, evidence is accumulating that increased hepatic copper concentration is primarily the result of dogs eating pet food with increased amounts and increased bioavailability of copper. Certain breeds seem to be predisposed (e.g. Labrador retrievers), which suggests an interaction between increased dietary copper and genetics. To date, no genetic marker for susceptibility to copper accumulation has been found in any breed other than the Bedlington Terrier (Johnston, et al 2013). In this case, while there is no overt necroinflammatory lesion, it is probable that the significant copper accumulation is causing oxidative stress and damage to hepatocytes, exacerbating the injury.

As of writing this report, this dog is reported to be doing well clinically. Low-dose dexamethasone suppression testing did not indicate hyperadrenocorticism, and coagulation studies did not reveal an overt hypercoagulable state. The dog is currently being managed on Denamarin, ursodiol, and penicillamine for chelation therapy. The submitting veterinarian and owner report the dog is clinically normal.

REFERENCES:

- Bayraktar UD, Seren S, Bayraktar Y (2007). 'Hepatic venous outflow obstruction: Three similar syndromes'. *World J Gastroenterol* 13(13): 1912-1927.
- Ferral H, Behrens G, and Lopera J (2012). 'Budd-Chiari Syndrome'. *AJR* 199: 737-745.
- Grooters AM and Smeak DD (1995). 'Budd-Chiari-like syndromes in dogs'. In: *Kirk's Current Veterinary Therapy XII*. Eds J. D. Bonagura and R. W. Kirk. W. B. Saunders, Philadelphia. pp 876-879
- Gulcubuk A, Bozkurt ER, and Erturk M (2012). 'Case report: Budd-Chiari-Like syndrome in a dog'. *Revue Méd. Vét.* 163(1): 7-10.
- Johnston AN, Center SA, McDonough SP, and Warner KL (2009). 'Hepatic copper concentrations in Labrador Retrievers with and without chronic hepatitis: 72 cases (1980-2010)'. *J Am Vet Med Assoc.* 242(3):372-380
- Menon KVN, Shah V, and Kamath PS (2004). 'The Budd-Chiari Syndrome'. *N Engl J Med* 350: 578-585.
- Otto CM, Mahaffey M, Jacobs C, and Binhasim A (1990). 'Cor triatrium dexter with Budd-Chiari Syndrome and a review of ascites in young dogs.' *JSAP* 31: 385-389.
- Patel RK, Lea NC, Heneghan, MA, Westwood, NB, et al (2006). 'Prevalence of the Activating JAK2 Tyrosine Kinase Mutation V617F in the Budd-Chiari Syndrome'. *Gastroenterology* 130(7): 2031-2038.
- Plessier A and Valla D-C (2008). 'Budd-Chiari Syndrome'. *Seminars in Liver Disease* 28(3): 259-269.
- Schoeman JP and Stidworthy MF (2001). 'Budd-Chiari-like syndrome associated with an adrenal pheochromocytoma in a dog.' *JSAP* 42: 191-194.
- Sepesy LM, Center SA, Randolph JF, Warner KL, and Erb HN (2006). 'Vacuolar hepatopathy in dogs: 336 cases (1993-2005). *JAVMA* 229: 246-252.
- Zimmerman MA, Cameron AM, and Ghobrial RM (2006). 'Budd-Chiari Syndrome'. *Clin. Liver Dis:* 259-273.

ACKNOWLEDGEMENTS:

We would like to thank Dr. Michael Koch for submission of this case to the surgical pathology service and Drs. Sharon A. Center and Sean McDonough for their comments on this case. We would also thank the histopathology staff at the Cornell University College of Veterinary Medicine, especially Aziza Solomon for trimming of this case, and the residents and faculty of the Section of Anatomic Pathology.

NEVPC Case #3
Slide #: 16-3129-1

Contributors: Olivia M. Swartley and John M. Cullen
Institution: North Carolina State University

Signalment: 2.5-year-old, spayed female, American Cocker Spaniel

History: The animal presented to the NCSU Internal Medicine Service for progressive lethargy, hypoproteinemia, and ascites. The animal initially reported to the referring veterinarian with urinary complaints and an enlarged abdomen. Abdominal radiographs at that time revealed poor serosal detail. Approximately 2 liters of a peritoneal transudate was drained. Bloodwork revealed mild neutrophilia, low normal BUN, moderate hypoalbuminemia, hypocholesterolemia, elevated GGT, and an inactive urine sediment and USG of 1.005. At NCSU, an ultrasound was performed revealing multiple extrahepatic portosystemic shunts and diffuse hepatopathy. Aspirates of the liver had extremely low cellularity with rare hepatocytes seen but no evidence of neoplasia. Biopsies were recommended but declined. Supportive treatment was pursued; however, the animal continued to decline. Euthanasia was elected and the animal was submitted for necropsy.

Gross findings: The abdominal cavity contained approximately 300 mL of yellow, mildly turbid fluid. Within the peritoneal cavity, there are many small to medium sized, tortuous, congested vessels that arise from the portal vein and communicate with the mesentery, kidneys, and pancreas. The liver was decreased in size, weighing 169 g (1.9% of total body weight, normal is 3-4%) and slightly pale and firm. Throughout all liver lobes, there were, multifocal, well-demarcated, smooth, raised, nodules that were similar in color to the adjacent parenchyma and vary in size from pinpoint to 4 cm in diameter. On cut section, the nodules extend into the underlying parenchyma.

Histopathology:

Liver: Affecting nearly 100% of two sections and approximately 30% of another section, the normal hepatic lobular architecture is disrupted and lost due to marked dissection along the sinusoids by a mixed population of myofibroblasts and mixed inflammatory cells (lymphocytes, plasma cells, histiocytes, and fewer neutrophils) within an eosinophilic, fibrillar collagenous matrix. Numerous scattered hemosiderin-laden Kupffer cells are also present. This dissecting fibrosis and mixed cellular infiltrate is markedly disrupting normal lobular and hepatic cord architecture and separating hepatocytes into scattered individual cells and multiple small clusters. Hepatocyte anisokaryosis is moderate with multifocally scattered karyomegaly seen. Hepatocytes are also frequently binucleated. Scattered hepatocytes occasionally contain multiple small, discrete, clear intracytoplasmic lipid-type vacuoles. Hepatocytes also occasionally contain a small amount of pale brown-yellow, granular intracytoplasmic pigment (interpreted as lipofuscin). Bile canaliculi are frequently filled with orange, linear to anastomosing pigment (bile plugs). Both within portal areas and also randomly throughout the disorganized/disrupted parenchyma, there are mildly increased numbers of small caliber bile ducts (ductular reaction). Multifocally, the hepatic architecture is disrupted by variably sized, well-demarcated, unencapsulated nodules, slightly compressive, nodules of regeneration. These nodules are characterized by well-differentiated hepatocytes forming hepatic cords, sometimes organized into a fairly normal lobular architecture around a central vein; however, decreased numbers of portal tracts are present. Within these nodules of regeneration, there are small foci of coagulative necrosis with a marked yellow-brown tinge to the stain of these necrotic hepatocytes (bile infarcts).

Morphologic Diagnosis:

1. Liver: marked, diffuse, dissecting fibrosis and chronic lymphohistiocytic hepatitis with canalicular bile plugging, ductular reaction, anisokaryosis, multifocal nodular regeneration, and bile infarcts
2. Abdominal cavity: moderate peritoneal effusion with multiple acquired extrahepatic portosystemic shunts

Discussion: The gross and histologic lesions in this animal are consistent with lobular dissecting hepatitis. Lobular dissecting hepatitis is a form of cirrhosis that affects juvenile and young adult dogs less than 5 years of age (average age is two years old). The American Cocker Spaniel breed is over represented with other affected breeds including the Standard poodle, Rottweiler, German shepherd, and Golden retriever. The disease is characterized histologically by loss of the lobular parenchyma by dissecting reticulin and fine collagen fibers that disrupt and individualize hepatocytes. A variable amount of mixed inflammatory cell infiltrates may also be present but portal inflammation and periportal fibrosis are not a conspicuous feature. Regenerative nodules may be present.

Young dogs typically present within signs related to synthetic hepatic failure, including ascites, weight loss, anorexia, diarrhea, vomiting, polydipsia, acquired portosystemic shunts, and/or jaundice. These patients are frequently hypoalbuminemic with elevated liver enzymes. An underlying etiology remains unknown; however, reports of similarly affected dogs from the same litter and household suggest both genetic and/or common etiologic sources. Disease progression is rapid with a poor prognosis and short survival time.

Acknowledgments: Joanna Barton and the NCSU Histology Laboratory

References

1. Cullen, JC and Stalker, MJ. Liver and Biliary system. In: Maxie MG, ed. Jubb, Kennedy, and Palmer's Pathology of Domestic Animals. Vol 2. 4 th Edition. St. Louis, MO: Elsevier; 2016: 305.
2. Cullen JM, van den Ingh TSGAM, Van Winkle T, Charles JA, Desmet VJ. Morphological classification of parenchymal disorders of the canine and feline liver. In: Rothuizen J, Bunch SE, Charles JA, et al., eds. WSAVA Standards for Clinical and Histological Diagnosis of Canine and Feline Liver Disease. eds. Philadelphia, PA: Saunders Elsevier; 2006: 97-98.
3. van den Ingh, TSGAM., and J. Rothuizen. "Lobular dissecting hepatitis in juvenile and young adult dogs." *Journal of Veterinary Internal Medicine* 8.3 (1994): 217-220.
4. Kanemoto, H., et al. "American cocker spaniel chronic hepatitis in Japan." *Journal of Veterinary Internal Medicine* 27.5 (2013): 1041-1048.
5. Mizooku, Hiroko, et al. "Histological and immunohistochemical evaluations of lobular dissecting hepatitis in American cocker spaniel dogs." *Journal of Veterinary Medical Science* 75.5 (2013): 597-603, 597-603.
6. Rothuizen, Jan. *WSAVA standards for clinical and histological diagnosis of canine and feline liver disease*. Elsevier Health Sciences, 2006.

2018 Northeast Veterinary Pathology - Gaithersburg, Maryland

April 7-8, 2018

NEVPC Case #4

Case Submission Form

Contributor (s) Institution: Esther Crouch DVM, MVS; Mason Jager, DVM; Andrew Miller, DVM, DACVP; Cornell University

Signalment: 14 year-old, female intact, Egyptian fruit bat (*Rousettus aegyptiacus*)

History:

A zoo collection Egyptian fruit bat was found on the ground of its enclosure two days in a row. The animal would climb back up only to feed. On physical examination the bat was in thin body condition with a body weight of 88 g (normal 100 – 120 g). Palpation revealed an enlarged liver. Abdominal ultrasound demonstrated a heterogenic liver with possible cavitation. Radiographs supported the finding of hepatomegaly. The bat was euthanized due to poor prognosis.

Gross Findings:

Major gross findings included marked hepatomegaly (7.0 g; 8.2% BW) with multifocal variably sized foci of discoloration scattered throughout all lobes. Additionally, multiple masses were present throughout all liver lobes that were distinct from the regions of discoloration. The gastric lymph nodes were moderately enlarged. In the lung, four distinct nodules with a similar consistency and color to the hepatic masses were noted.

Histopathologic/Cytologic Findings:

Liver: Multifocally throughout the parenchyma and affecting up to 70% of some sections are multiple irregularly round, infiltrative to expansile masses composed of polygonal epithelial cells forming disorganized, anastomosing cords and trabeculae up to five cells thick, megacanalculi, and sheets (neoplastic hepatocytes). The cells have distinct cell margins and moderate amounts of eosinophilic granular cytoplasm with variable vacuolation (glycogen, presumptive). The nuclei are central with sparse chromatin and prominent peripheral nucleoli (hepatocytes). There is moderate anisocytosis and anisokaryosis with occasional bizarre nuclei. A mitotic rate of 16 mitoses in ten 400X high powered fields is noted. Throughout the sinusoids are moderate numbers of macrophages containing large amounts of variably sized brown pigmented cytoplasmic granules (hemosiderin, presumptive). Acini occasionally contain yellow-green material (bile, presumptive) and occasional round aggregates of yellow-green material are seen between hepatocytes (canalicular biliary cholestasis).

Tongue and eye sections are within normal limits.

The following histochemical stains were applied to liver:

Reticulin-stain for extracellular structural proteins: Staining of reticulin fibers in hepatocellular basement membranes highlights loss of normal hepatic cord architecture in areas of tumor growth and compression of the adjacent parenchyma with some evidence of parenchymal extinction in the subcapsular areas.

Masson's trichrome for fibrillar collagen: The stain highlights fine bands of fibrosis that separate trabeculae of neoplastic cells.

Prussian blue for iron: Stainable iron is present in small to moderate amounts of granular and fine intracytoplasmic iron of hepatocytes and moderate to large amounts of dense granular iron in all Kupffer cells in non-neoplastic regions with an absence of iron in neoplastic regions.

Morphologic/Etiologic Diagnosis:

Liver:

1. Hepatocellular carcinoma
2. Hemosiderosis

Lungs and gastric lymph nodes: Metastatic hepatocellular carcinoma (slides of these sections not submitted for NEVPC)

Discussion:

The presence of multiple masses in the liver and lungs, as well as gastric lymphadenopathy, are indicative of a neoplastic process. The gross appearance, histologic features, signalment, and clinical history are consistent with the diagnosis of hepatocellular carcinoma with metastasis. Histochemical analysis of the liver with Prussian blue, a stain that highlights iron, demonstrates a significant accumulation of iron in hepatocytes and Kupffer cells in the regions of parenchyma unaffected by neoplasia. In these non-neoplastic regions there does not appear to be evidence of tissue remodeling or fibrosis, consistent with hemosiderosis rather than hemochromatosis. The distinction lies in whether there is evidence of tissue destruction associated with the iron accumulation, which is termed hemochromatosis.

In 2016, Leone et al. reported that hemochromatosis, a well-documented and prevalent disease in captive populations of the Egyptian fruit bat, is associated with development of neoplasia.⁸ In this study hepatocellular carcinoma was the most common tumor associated with hemochromatosis and metastasis to the lungs was described. Cholestasis, extravascular fluid accumulation, and icterus were commonly reported as causes of death or euthanasia.⁸ Iron overload in Egyptian fruit bats is a disease of captivity and has largely been attributed to diets containing excessive iron. It appears that within Chiroptera, this is a disease unique to this species and related to their high degree of efficiency in dietary iron uptake.⁴ Presumably, the diet they are accustomed to in the wild contains minimal iron and this is a useful adaptation. At least one free-ranging study of Egyptian fruit bats has observed feeding on plants containing high concentrations of tannins.⁷ Tannins inhibit iron absorption. Conversely, vitamin C acts to increase non-heme iron absorption from dietary sources and may potentiate free radical damage

within tissues due to iron accumulation.^{2,5} Dietary restriction of vitamin C is problematic in a species so reliant on fruit food stuffs.

The correlation between hemochromatosis and HCC has been convincingly demonstrated; however, the exact mechanism of neoplastic induction has not been elucidated. HCC is a common sequelae to human hereditary hemochromatosis, and within this sphere of research debate continues as to whether the increased concentration of iron is by itself carcinogenic, or whether the HCC develops secondary to the hepatic damage caused by the excessive iron.^{8,9} Most commonly, HCC development in humans is seen within cirrhotic livers; however, there is a rare subset of humans with hemochromatosis in which HCC development is seen in the absence of cirrhosis and associated fibrosis and remodeling.⁹ This suggests that iron accumulation may induce neoplasia independent of concurrent cirrhosis. Humans with hemochromatosis have also been shown to have increased production of reactive oxygen species (ROS).^{6,8} The cumulative effect of ongoing DNA damage resultant from ROS injury associated with increased iron concentrations may underlie mutagenesis that precede HCC development.^{6,8} This has certainly been demonstrated in rat models.¹

Human and Egyptian fruit bats are not alone in their development of hemochromatosis, a variety of captive bird and mammalian species are also susceptible; browsing rhinoceroses, (*Diceros bicornis*, *Dicerorhinus sumatrensis*), red deer (*Cervus elaphus*), Salers cattle (*Bos taurus*), lemurs (*Eulemur macaco*, *E. fulvus*, *E. coronatus*, *Lemur catta*, *Varecia variegata variegata*, *V. variegata ruber*, *Propithecus verreauxi coquereli*), horses (*Equus caballus*), tapirs (*Tapirus bairdii*, *Tapirus indicus*, *Tapirus terrestris*), rock hyrax (*Procavia capensis*), mynahs (*Gracula religiosa*, *Leucospiza rothschildi*), toucans (*Ramphastos toco*), and tanagers (*Ramphocelus carbo*, *Stephanophorus dia dematus*, *Tangara arthus*, *Tangara icterocephala*, *Thraupis bonariensis*, *Thraupis episcopus*).^{4,8} An association with hemochromatosis and hepatocellular carcinoma is yet to be made in these species. HCCs are a relatively rare neoplasm in most species and largely exhibit benign behavior. These infrequently metastasize with spontaneous rupture a much more frequent cause of morbidity and mortality in HCC affected animals.³ Egyptian fruit bat iron-associated HCC are unique in their propensity to induce liver failure and metastasis. Similarly malignant HCCs are seen with some frequency in captive prosimian species, however, a recent study did not find a correlation between HCC incidence and iron levels.¹⁰

In this case, we theorize that the hemosiderosis contributed to the development of HCC. We are also aware that areas of the liver that would have been consistent with hemochromatosis, may have been masked by the proliferation of the HCC.

Acknowledgements:

I would like to thank Dr. Noha Abou-Madi for submission of this case to the necropsy service. I am also grateful to the histopathology staff at the Cornell University College of Veterinary Medicine for their assistance.

References:

- 1 Asare GA, Mossanda KS, Kew MC, Paterson AC, Kahler-Venter CP, Siziba K: Hepatocellular carcinoma caused by iron overload: A possible mechanism of direct hepatocarcinogenicity. *Toxicology* 2006;219(1):41-52.
- 2 Cook JD, Watson SS, Simpson KM, Lipschitz DA, Skikne BS: The effect of high ascorbic acid supplementation on body iron stores. *Blood* 1984;64(3):721-726.
- 3 Cullen J, Stalker MJ: Liver and Biliary System. In: Maxie MG, ed. *Jubb, Kennedy, and Palmer's Pathology of Domestic Animals*. sixth ed. Missouri: Elsevier; 2016: 345-347.
- 4 Farina LL, Heard DJ, LeBlanc DM, Hall JO, Stevens G, Wellehan JFX, et al.: Iron Storage Disease in Captive Egyptian Fruit Bats (*Rousettus aegyptiacus*): Relationship of Blood Iron Parameters to Hepatic Iron Concentrations and Hepatic Histopathology. *Journal of Zoo and Wildlife Medicine* 2005;36(2):212-221.
- 5 Herbert V, Shaw S, Jayatilleke E: Vitamin C-driven free radical generation from iron. *The Journal of Nutrition* 1996;126(Supplement):1213S-1220S.
- 6 Jomova K, Valko M: Advances in metal-induced oxidative stress and human disease. *Toxicology* 2011;283(2-3):65-87.
- 7 Korine C, Izhaki I, Arad Z: Is the Egyptian fruit-bat *Rousettus aegyptiacus* a pest in Israel? An analysis of the bat's diet and implications for its conservation. *Biological Conservation* 1999;88(3):301-306.
- 8 Leone AM, Crawshaw GJ, Garner MM, Frasca S, Stasiak I, Rose K, et al.: A retrospective study of the lesions associated with iron storage disease in captive Egyptian fruit bats (*Rousettus aegyptiacus*). *Journal of Zoo and Wildlife Medicine* 2016;47(1):45-55.
- 9 Von Delius S, Lersch C, Schulte-Frohlinde E, Fend F, Dobritz M, Schmid R, et al.: Hepatocellular carcinoma associated with hereditary hemochromatosis occurring in non-cirrhotic liver. *Zeitschrift für Gastroenterologie* 2006;44(01):39-42.
- 10 Zadrozny L, Williams C, Remick A, Cullen J: Spontaneous hepatocellular carcinoma in captive prosimians. *Veterinary Pathology* 2010;47(2):306-311.

NEVPC Case #5
Slide #: 18-298

Contributors: Elizabeth C. Alloway, John M. Cullen
Institution: North Carolina State University

Signalment: 8 week old, intact female, Labradoodle

History: The puppy was presented to the North Carolina State University Small Animal Emergency Service for evaluation of lethargy and vomiting. Initial evaluation by the referring veterinarian revealed a fever (T: 104.1°F) and dehydration; medical management with antibiotics, subcutaneous fluids, and deworming was attempted prior to presentation but the puppy's symptoms did not improve.

On physical examination, the puppy was in lateral recumbency, with a depressed but responsive mentation. She was mildly hypothermic (T: 99.4°F) with white mucous membranes and an undetectable capillary refill time. No ocular discharge, corneal edema, or aqueous flare was noted on ophthalmic examination. Petechia were observed on the inguinal skin, external ear canals, and along the clipped skin.

A complete blood count also revealed a mild leukopenia (total WBC count of 4.44×10^3 cells/ μ L, reference range: $4.39 - 11.61 \times 10^3$ cells/ μ L) with a mild neutropenia (2.043×10^3 cells/ μ L, reference range $2.841 - 9.112 \times 10^3$ cells/ μ L) with a left shift (bands 1.243×10^3 cells/ μ L, reference range: 0×10^3 cells/ μ L), moderate lymphopenia (0.188×10^3 cells/ μ L, reference range: $.594 - 3.305 \times 10^3$ cells/ μ L), and a marked thrombocytopenia (14×10^3 cells/ μ L, reference range: $190 - 468 \times 10^3$ cells/ μ L). The dog's PCV was 12%; the anemia was noted to be non-regenerative (reticulocyte count 1000 cells/ μ L, reference range: $.11 - 1.26 \times 10^3$ cells/ μ L), normocytic, and normochromic.

Serum chemistry panel and serum ammonia were consistent with synthetic liver failure, with a hepatocellular injury pattern (ALT 1658IU/L, reference range: 12 – 54IU/L; ALP 829 IU/L, reference range: 16 – 140IU/L), a serum glucose of 12mg/dL (reference range: 70 – 131 g/dL), serum albumin of 1.7g/dL (3 - 3.9g/dL), total bilirubin of 1.6mg/dL (<0.2 mg/dL), and serum ammonia of 379 μ mol/L (<30 μ mol/L). A coagulation panel revealed markedly prolonged clotting times (PT – 48 seconds, APTT >120 seconds), elevated D-dimers (1100 ng/mL), and decreased serum fibrinogen (32 mg/dL), consistent with disseminated intravascular coagulation.

A parvovirus SNAP test was performed and was negative.

The dog was treated for hypoglycemia, shock, and DIC with fluids, fresh frozen plasma, and packed red blood cells. Due to lack of response, progressive deterioration, and poor prognosis, the dog was euthanized.

Gross findings:

Liver: Diffuse, moderate hepatomegaly (7% body weight) with diffuse pallor, multifocal to coalescing petechial to ecchymotic hemorrhages, and focal fibrinous serositis

Gall bladder: Moderate, diffuse, transmural edema

Esophagus, stomach; Moderate luminal hemorrhage and multifocal to coalescing petechial serosal hemorrhages

Brain, left temporal lobe: Mild, focal leptomenigeal hemorrhage

Lungs: Mild to moderate, multifocal to coalescing hemorrhage and edema

Histopathology:

Liver: Two sections are examined. Affecting approximately 75% of the parenchyma in one section and 30% in the second section, there is moderate to marked, multifocal to coalescing, centrilobular to midzonal to rare panlobular coagulative to lytic necrosis and hemorrhage. Necrotic hepatocytes (shrunken with irregular cell margins, hypereosinophilic cytoplasm, and pyknotic to karyorrhectic nuclei) are frequently observed within the regions of hemorrhage, with rare admixed neutrophils and small amounts of fibrin. Hepatocytes at the margins of the affected to unaffected regions exhibit hydropic degeneration to necrosis. Frequently, necrotic and viable hepatocytes as well as sinusoidal lining cells contain a single large (2-3µm), deeply basophilic viral intranuclear inclusion body, with marginalization of the nuclear chromatin. Within the small amount of remaining viable parenchyma, there are occasional binucleated hepatocytes, rare mitotic figures, and multifocal Kupffer cell hyperplasia. In regions with intact central veins, the venous endothelia is mildly hypertrophied and the adventitia is expanded by edema, small amounts of hemorrhage and fibrin, mild numbers of lymphocytes and macrophages. Infiltrating the portal tracts are mild numbers of lymphocytes and macrophages, with mild expansion of the adventitia by perivascular hemorrhage and edema. Lymphocytes rarely intercalate with the biliary epithelium and there is mild, multifocal vacuolation of the biliary epithelium. Portal lymphatics are mildly to moderately distended.

Morphologic Diagnosis:

Liver: Marked, centrilobular to midzonal, acute, coagulative to lytic necrosis with hepatocyte, and sinusoidal lining intranuclear inclusion bodies, hemorrhage, and mild lymphohistiocytic hepatitis

Additional lesions in other tissues include:

1. Lymphoid tissue (hepatic lymph node > pancreatic lymph node > pharyngeal tonsil > colonic peyer's patches > spleen): Moderate, multifocal lymphocytolysis with histiocytic hyperplasia, and variable hemorrhage
2. Pharyngeal tonsil: Mild to moderate, multifocal, keratinocyte necrosis with intranuclear inclusions
3. Gall bladder: mural edema, diffuse, severe
4. Lung: pulmonary edema (gross) and mild, multifocal alveolar histiocytosis with uncommon alveolar septal intranuclear inclusion bodies
5. Bone marrow:
 - a. Moderate, multifocal to coalescing hemorrhage
 - b. Moderate, multifocal to coalescing histiocytosis
 - c. Myeloid hyperplasia, mild with left shifting
 - d. Megakaryocytic hyperplasia, mild with left shifting
6. Small intestine:
 - a. Mild, multifocal, crypt enterocyte necrosis
 - b. Moderate luminal hemorrhage
7. Kidney: Minimal, multifocal, glomerular tuft intranuclear inclusion bodies
8. Pancreas: Mild to moderate, multifocal acute interlobular hemorrhage
9. Large intestine: Mild larval nematodiasis
10. Brain: Severe, diffuse congestion

Immunohistochemistry

Immunohistochemical preparations for Canine Adenovirus type 1 and 2 were applied to the sections of liver, spleen, lung, and kidney. Positive and negative controls stained appropriately with minimal background staining. Numerous hepatocytes, sinusoidal lining cells (suspected Kupffer cells and sinusoidal endothelia), pulmonary interstitial endothelium, glomerular endothelium have strong, intranuclear and intracytoplasmic immunoreactivity, consistent with canine adenovirus infection.

Discussion:

Infectious canine hepatitis is caused by Canine adenovirus 1 (CAvV-1), which is a non-enveloped, double-stranded DNA virus. CAvV-1 is highly stable within the environment, where it is resistant to chemicals such as chloroform, ether, acid, formalin, and some frequencies of ultraviolet radiation. Clinical disease is noted in a variety of species, including dogs, coyotes, foxes, wolves, other canids, bears, and otters. Transmission may occur from contact with infected secretions (including nasal discharge, blood, saliva, urine, and feces), fomites, and contaminated soil.

CAvV-1 infection typically originates in the oronasal cavity: the virus then localizes in the tonsils and spreads via the regional lymph nodes and lymphatics to the thoracic duct and systemic blood circulation. CAvV-1 exhibits tropism for endothelium, mesothelium, and hepatic parenchyma including Kupffer cells. Classic pathologic features are related to direct cytotoxicity and include centrilobular to massive hepatic necrosis, serosal hemorrhage, and gall bladder edema.

Affected patients are typically less than 1 year of age; however, unvaccinated dogs of any age may be infected and exhibit clinical signs. In the early stage of disease, fever, tachypnea, and tachycardia are noted in conjunction with tonsillar enlargement, pharyngitis, and laryngitis. As the disease progresses, clinical signs are referable to hepatic necrosis and endothelial injury. These include mucosal petechia, pale, icteric mucous membranes, vomiting, melena, abdominal pain, and fever. In dogs who survive beyond the initial hepatic necrosis, proteinuria may develop due to renal tubular infection. Additionally, as recovery is initiated, dogs may develop a type III hypersensitivity response, with immune complex deposition on the corneal endothelium and free within the vitreous fluid. Clinically, this manifests as an anterior uveitis and corneal edema ("blue eye").

Clinical diagnostic findings of CAvV1 include hematologic and biochemical abnormalities. Early hematologic abnormalities include leukopenia with lymphopenia and neutropenia; recovering dogs will typically exhibit a lymphocytosis (with an increased number of activated lymphocytes) and neutrophilia. Biochemical abnormalities may include a mild hyperglobulinemia, elevated activities of ALT, AST, ALP, and bilirubin, and proteinuria. Abnormalities in serum fibrin concentration, elevated D-Dimers, thrombocytopenia, and prolonged clotting times may be observed in patients experiencing DIC. CSF may be normal or exhibit a mononuclear pleocytosis due to a lymphoplasmacytic encephalitis.

In affected patients, the liver is grossly mildly enlarged and friable, with a mild fibrinous serositis and mild icterus. The gall bladder is classically moderately thickened by edema. Superficial lymph nodes may be edematous, congested, and hemorrhagic. Multifocal hemorrhage and hemorrhagic infarction is documented affecting the renal cortices, lungs, brain (midbrain and brainstem), and metaphysis of long bones as well as suffusive serosal hemorrhage throughout the gastrointestinal tract.

Typical hepatic histologic lesions include centrilobular zonal coagulative to lytic necrosis with replacement by sinusoidal dilation and hemorrhage. Basophilic intranuclear inclusion bodies within necrotic and viable hepatocytes as well as endothelia and Kupffer cells. Hydropic degeneration and fatty change are commonly observed. A mild lymphoplasmacytic hepatitis may be observed. Within other organs, lesions are variable and dependent upon infection of the endothelium. Hemorrhage, edema, and fibrin are found in multiple organs, including the kidney, lung, and brain; intranuclear viral inclusions may be found in the endothelium of these organs. Within cases of "blue eye", plasmacytic and neutrophilic infiltration as well as edema may be observed within the iris, ciliary body, filtration angle, and cornea.

Treatment for CAdV1 is typically supportive, with the goals of maintaining hydration status, electrolyte balance, and normal coagulation status. Medications to counteract hyperammonemia may decrease signs of hepatoencephalopathy.

In contrast to CAdV1, CAdV2 exhibits tropism for the respiratory epithelium. Clinical signs associated with CAdV2 include tonsillitis, cough, and respiratory distress. Antemortem diagnostics include virus isolation, indirect hemagglutination assay, complement fixation, immunodiffusion, and ELISA. Diagnosis of CAdV1 infection and differentiation between infection with CAdV1 and CAdV2 has been documented with PCR techniques in a variety of species including dogs, a Euroasian river otter, red foxes, and raccoons.

Prevention of both conditions is largely through maternal antibodies in young puppies and parenteral administration of a series of modified live CAdV2 vaccines as maternal antibodies wane. Modified live CAdV1 vaccines have historically provided adequate immunity to CAdV1 infection; however, post vaccinal complications were common and included subclinical interstitial nephritis, anterior uveitis, pyrexia, and tonsillar enlargement. As such, CAdV1 vaccines are no longer recommended and there is limited widespread availability.

References:

1. Cullen, JC and Stalker, MJ. Liver and Biliary system. In: Maxie MG, ed. *Jubb, Kennedy, and Palmer's Pathology of Domestic Animals*. Vol 2. 4th Edition. St. Louis, MO: Elsevier; 2016. 310-312.
2. Greene, CE. Infectious Canine Hepatitis and Canine Acidophil Cell Hepatitis. In: Greene's *Infectious Diseases of the Dog and Cat*. 4th Edition. 42-48.
3. Cullen JM, van den Ingh TSGAM, Van Winkle T, Charles JA, Desmet VJ. Morphological classification of parenchymal disorders of the canine and feline liver. In: Rothuizen J, Bunch SE, Charles JA, et al., eds. *WSAVA Standards for Clinical and Histological Diagnosis of Canine and Feline Liver Disease*. eds. Philadelphia, PA: Saunders Elsevier; 2006:91.
4. Park, NY, Lee, MC, Kurkure, NV and Cho, HS. Canine adenovirus type 1 infection of a Eurasian river otter (*Lutra lutra*). *Vet Pathol*. 2007; 44: 536-539.
5. Chouinard L, Martineau D, Forget C, et al. 1998. Use of polymerase chain reaction and immunohistochemistry for detection of canine adenovirus type 1 in formalin-fixed, paraffin-embedded liver of dogs with chronic hepatitis or cirrhosis. *J Vet Diagn Invest* 10:320-325.
6. Hechinger, S., Scheffold, S., Hamann, HP., Zsochock, M. Detection of canine adenovirus 1 in red foxes and raccoons in Germany with a TaqMan real-time PCR assay. *JVDI*. 2017; 29: 741-746.

1060 William Moore Drive
Raleigh, NC 27607

919.513.6240 (Department Head
Administrative Office)
919.513.6464 (Fax)

Acknowledgments: Dr. Laura Chen, Joanna Barton and the NCSU Histology Laboratory, and Dr. Allison Tucker and the Rollins Animal Disease Laboratory (North Carolina Veterinary Diagnostic Laboratory System).

NEVPC 2018

Case #6

CONTRIBUTOR(S)/INSTITUTION: Jolie Demchur, University of Pennsylvania

SIGNALMENT: Multiple white-tailed deer (*Odocoileus virginianus*) neonatal to juvenile fawns.

HISTORY: As part of an ongoing investigation into fawn mortality in southern Delaware, 79 white-tailed deer neonates were captured shortly after birth, tagged and affixed with high frequency radio collars. The fawns were monitored and carcasses were collected if a mortality signal was received. Of the 79 fawns captured and tagged, 25 (32%) were found deceased. A total of 21 carcasses had sufficiently intact viscera for complete gross and histologic evaluation. Clinical signs were not observed, physical examination and antemortem diagnostics were not performed in any cases.

GROSS FINDINGS: Of the 21 animals examined, a small group of 6 fawns exhibited similar gross and/or histologic lesions. All fawns had numerous ixodid ticks adhered to the skin, concentrated around the head and pinnae. Visceral and subcutaneous adipose tissue was scant to absent in all fawns. In some cases, the epicardial fat was atrophied and replaced by clear gelatinous tissue (serous atrophy). Three fawns had mild to severe icterus throughout the skin, subcutis and viscera. In multiple fawns, the hepatic parenchyma contained multifocal random pinpoint white foci. Concurrent lesions included regional necrotizing pulmonary thromboarteritis and pneumonia, fibrinosuppurative pleuropneumonia, oral and ruminal necrobacillosis.

HISTOPATHOLOGIC/CYTOLOGIC FINDINGS:

Sections of liver from multiple animals exhibited a variety of lesions. Tissue from 4 fawns contained markedly enlarged leukocytes ranging from 50-300 µm in diameter with abundant pale eosinophilic foamy to vacuolated cytoplasm and elongate, serpentine to lobulated nuclei with numerous prominent nucleoli. The cytoplasm of the enlarged leukocytes was distended with innumerable 1-2 µm in diameter irregularly round basophilic protozoan parasites (megashizonts/megameronts). In three of these animals, the enlarged leukocytes were multifocally ruptured, with release of myriad round to ovoid 1-2 µm in diameter basophilic merozoites into the adjacent tissue. Ruptured leukocytes and free merozoites were surrounded by neutrophils and fewer macrophages admixed with fibrin, necrotic hepatocytes, karyorrhectic debris and occasionally, mineral. In two additional animals, the hepatic parenchyma contained similar multifocal random foci of necrosis and suppurative inflammation, although no organisms were detected in these fawns. Interestingly, these two animals also had multifocal degeneration and acute coagulative necrosis of centrilobular hepatocytes. Acute centrilobular necrosis was also observed in one fawn with intrahepatic organisms. The submitted slides contain additional tissues (adrenal gland, kidney) that did not exhibit significant lesions.

MORPHOLOGIC/ETIOLOGIC DIAGNOSIS:

Liver, white-tailed deer (*Odocoileus virginianus*): moderate multifocal random acute necrosuppurative hepatitis with intracytoplasmic and extracellular merozoites (consistent with *Theileria* spp.); mild multifocal acute centrilobular degeneration and necrosis

DISCUSSION:

Theileria spp. are apicomplexan protozoal hemoparasites transmitted by tick vectors that infect wild and domestic ungulates around the world. Pathogenicity varies greatly among *Theileria* spp., ranging from severe clinical disease with high morbidity and mortality (*T. parva*, *T. annulata*, *T. lestoquardi*) to mild or asymptomatic infections (*T. buffeli*).¹ Sporadic cases of bovine theileriosis have occurred in the southeastern United States, although many species of *Theileria*, including *T. parva* (agent of East Coast Fever) and *T. annulata* (cause of Mediterranean or tropical theileriosis) have not been detected in North America.² Theileriosis has also been reported in wild and domestic cervids in the southeastern United States. *Theileria cervi* was first identified in a white-tailed deer in 1962, and has since been reported in elk and mule deer.^{3, 4, 5, 6}

Theileria cervi is transmitted by Lone Star ticks (*Amblyomma americanum*) and is typically considered non-pathogenic. As in many *Theileria* spp., the life cycle of *T. cervi* includes both leukocytic and erythrocytic stages. Infected ticks transmit sporozoites in saliva while feeding on hosts. Sporozoites infect leukocytes through receptor-mediated phagocytosis. Macromeronts/macroschizonts develop within the cytoplasm of infected white blood cells, markedly enlarging the cell. Rupture of the host cell wall releases merozoites into the tissue, which then enter erythrocytes. The organisms develop into piroplasms in erythrocytes, and fission of the piroplasms can cause cell rupture.^{6,7} While *T. cervi* infections in white-tailed deer are most often subclinical, disease and mortality can occur in animals with a high parasite burden or with concurrent disease.⁴

In this group of animals, theileriosis was diagnosed based on the observation of markedly enlarged intrahepatic leukocytes distended with developing organisms. In most cases, a diagnosis of theileriosis is made by identifying intraerythrocytic piroplasms in Giemsa-stained whole blood smears. It is unusual to observe the macromeront/macroschizont or merozoite stages in tissue sections, as these stages are transient and only one cycle of merogony occurs after initial infection with sporozoites.⁶ Multiple *Theileria* spp. have similar meront, merozoite and piroplasm morphology, thus additional molecular diagnostics are required for speciation.⁷

In some of the fawns in this group, theileriosis was considered to be an incidental finding. However, concurrent icterus and acute centrilobular hepatic necrosis in three of the fawns provided evidence for a clinically relevant infection that likely contributed to mortality. Given the recent expansion of *Amblyomma americanum* population and range, it is possible that the incidence of *T. cervi* infections in the Mid-Atlantic and Northeastern regions will increase and may have implications for neonatal health and mortality.⁸

REFERENCES:

1. Valli VEO, Kiupel M, Bienzle D, Wood D. Hematopoietic system. In: Maxie MG, ed. Jubb, Kennedy, and Palmer's Pathology of Domestic Animals. 6th ed. Vol 3. Philadelphia, PA: Elsevier Sanders; 2016:176-177.
2. Stockham S, Kjemtrup A, Conrad P, et al. Theileriosis in a Missouri beef herd caused by *Theileria buffeli*: Case report, herd investigation, ultrastructure, phylogenetic analysis, and experimental transmission. *Vet Pathol.* 2000;37:11-21.
3. Kreier, J, Ristic, M, Watrach, A. *Theileria* sp. in a deer in the United States. *Am J Vet Res.* 1962;23:657-662.
4. Yabsley M, Quick T, Little S. Theileriosis in a white-tailed deer (*Odocoileus virginianus*) fawn. *J Wildl Dis.* 2005;41:806-809.
5. Chae J, Waghela S, Craig T, Kocan A, Wagner G, Holman P. Two *Theileria cervi* SSU rRNA Gene Sequence Types Found In Isolates From White-Tailed Deer And Elk In North America. *J Wildl Dis.* 1999;35(3):458-465.
6. Wood J, Johnson E, Allen K, Campbell G, Rezabek G, Bradway D, Pittman L, Little S, Panciera R. Merogonic stages of *Theileria cervi* in mule deer (*Odocoileus hemionus*). *J Vet Diagn Investig.* 2013;25: 662-665.
7. Mans B, Pienaar R, Latif A. A review of Theileria diagnostics and epidemiology. *Int J Parasitol Parasites Wildl.* 2015;4(1):104-118.
8. Springer Y, Jarnevich C, Barnett D, Monaghan A, Eisen R. Modeling the present and future geographic distribution of the lone star tick *Amblyomma americanum* (Ixodida: Ixodidae), in the continental United States. *Am J Trop Med Hyg.* 2015;93:875-890.

ACKNOWLEDGMENTS:

Thanks to Jacob Haus, Justin Dion and Jacob Bowman from the University of Delaware's department of Entomology and Wildlife Ecology for submitting the fawns as part of their investigation into fawn mortality in southern Delaware (funding provided by: Wildlife and Sportsfish Restoration grant from the U.S. Fish and Wildlife Services – award number F15AF00929, Delaware Department of Natural Resources and Environmental Control, and The U.S. Department of Agriculture National Institute of Food and Agriculture, Hatch project DEL00712 and McIntire Stennis DEL00672). Many thanks to Drs. Susan Bender and Perry Habecker (supervising pathologists) for their assistance with this case series.

C.L. Davis 2018
Northeastern Veterinary Pathology Conference

NEVPC Case #7

Contributor(s)/Institution:

Kathleen Mulka, DVM and Lisa Mangus, DVM, PhD, DACVP
Johns Hopkins University, School of Medicine
Department of Molecular and Comparative Pathobiology
Broadway Research Building, #811
733 N. Broadway
Baltimore, MD 21205
Phone: 443-287-2953
Fax: 443-287-5628

Signalment:

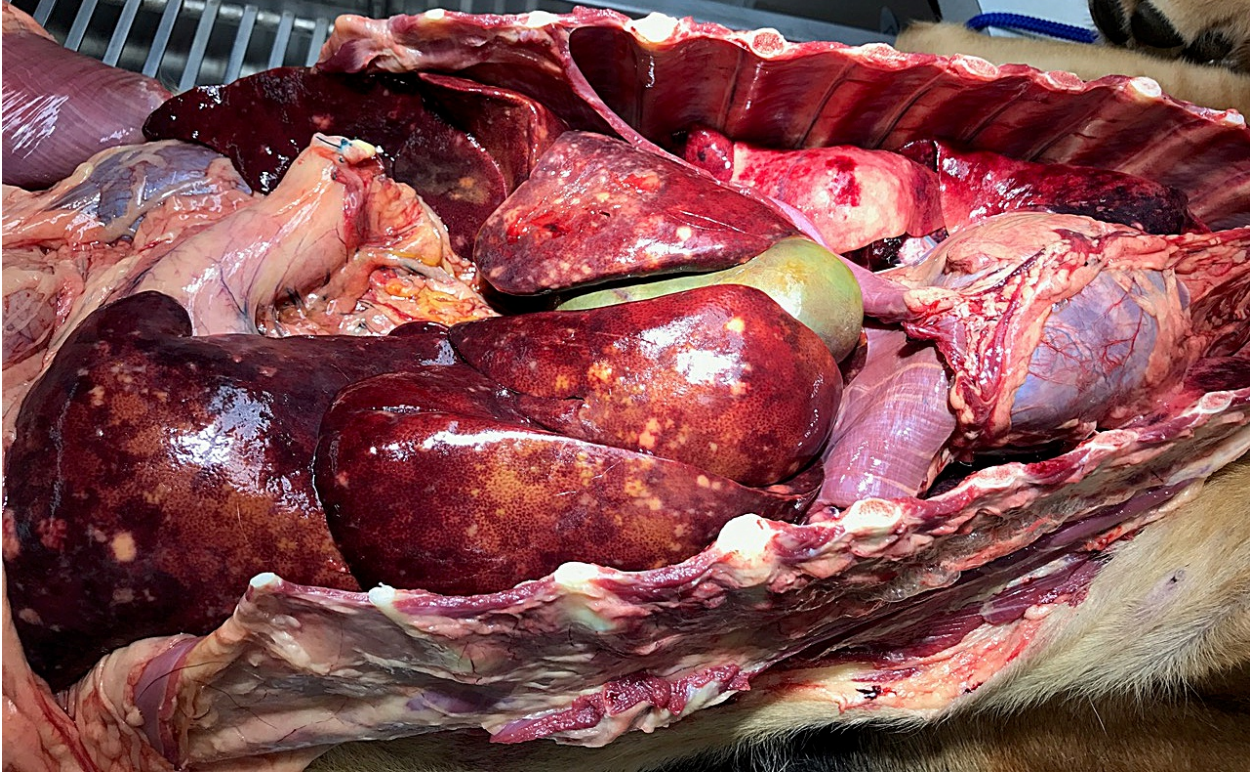
22 month old intact male bloodhound

History:

This animal was purchased from a breeder at 8 weeks of age. When the dog was 10 months old, he began exhibiting neurologic signs and was diagnosed with sterile meningitis, which was successfully managed with prednisone. Neurologic signs recurred 5 months later and the dog was again treated with prednisone. Due to food and environmental allergies, this dog also received cyclosporine chronically. In the week prior to necropsy, the dog exhibited rapid weight loss, progressive inappetence, and acute onset of fever. At presentation, serum chemistry revealed elevated liver enzymes (ALT 881 U/L, ALP 318 U/L) and globulins (5.2 g/dL). On CBC, total white blood cell count and differential were normal, but there were mild toxic changes to neutrophils (Doehle bodies), occasional bands, and reactive lymphocytes suggestive of inflammation. The dog also had moderate to marked thrombocytopenia and prolonged aPTT. A tick PCR panel was negative for all organisms. Fungal serology was negative for Coccidioides, Blastomycosis, Cryptococcus, Histoplasma, and Aspergillus. Three-view chest radiographs revealed interstitial infiltrates in the caudodorsal lung fields. On abdominal ultrasound, the liver appeared enlarged and slightly hyperechoic with rounded margins. Cytology of liver showed mild cholestasis with mixed inflammation; no infectious agents or neoplastic cells were identified. Despite intensive treatment including IV fluids, antibiotics, and oral fluconazole, the dog's condition deteriorated over 3-4 days and euthanasia was elected.

Gross Findings:

A partial necropsy was performed which revealed generalized ecchymosis and icterus. The liver was markedly enlarged and contained dozens of firm, pale-yellow nodules throughout all lobes. The lungs contained multiple similar nodules and were severely congested and hemorrhagic. The mediastinum was edematous with enlarged lymph nodes.



Histopathologic/Cytologic Findings:

Liver. There are multiple coalescing areas in which the hepatic parenchyma is disrupted and replaced by large numbers of inflammatory cells, necrotic cellular debris, fibrin, and streams of plump, reactive fibroblasts. The inflammatory infiltrates are predominantly composed of viable and degenerate neutrophils, fewer macrophages, and scattered lymphocytes and plasma cells. Macrophages often are expanded up to 30µm in diameter and contain numerous basophilic, 2-4 µm diameter, oval-shaped merozoites. Merozoites are occasionally arranged in rosettes within thin-walled schizonts. In areas adjacent to the inflammation and necrosis, there is variable sinusoidal congestion and hepatocytes are occasionally shrunken (atrophy) or swollen with cytoplasmic lipid vacuoles (degeneration). There is also multifocal periportal inflammation with moderate associated biliary hyperplasia.

Immunohistochemistry:

Toxoplasma gondii – no positive immunoreactivity

Neospora caninum – no positive immunoreactivity

Sarcocystis spp. (polyclonal against *S. neurona*) – intense positive staining of apicomplexan organisms

PCR:

Neospora spp. – negative

Sarcocystis spp. – positive; subsequent sequence analysis of PCR product showed 100% identity to *Sarcocystis neurona*

Morphologic Diagnosis: Liver: hepatitis, pyogranulomatous and necrotizing, multifocal to coalescing, severe, with intralesional intrahistiocytic merozoites and schizonts

Etiologic Diagnosis: Hepatic sarcocystosis

Cause: *Sarcocystis neurona*

Discussion:

Sarcocystis species are apicomplexan protozoan parasites that have a two-host life cycle consisting of an intermediate host and a definitive host. In most species of *Sarcocystis*, the intermediate hosts are herbivores and the definitive host are carnivores. *Sarcocystis spp.* are transmitted to the intermediate host through ingestion of sporocysts, oocysts, or both, in contaminated feed, soil, or water. Sarcocysts are formed in tissues, typically muscle or central nervous system, after schizogony. The definitive host becomes infected through ingestion of tissues with encysted sarcocysts.^{1,2}

Sarcocystis neurona is the organism most commonly associated with equine protozoal myeloencephalitis (EPM), a serious neurological disease in horses. Opossums are the definitive hosts. Hosts are considered aberrant if only schizonts are identified within tissues, as mature sarcocysts are required for completion of the life cycle. Proven intermediate hosts include the cat, skunk, raccoon, armadillo, and sea otter. Other reported intermediate hosts include brown-headed cowbirds. Reported aberrant hosts include the horse, pony, zebra, raccoon, red panda, cat, ferret, dog, skunk, lynx, sea otter, pacific harbor seal, sea lion, and fisher.¹

Dogs can be the definitive host of various species of *Sarcocystis*, and can be the intermediate and aberrant hosts as well.³ There are limited reports of *S. neurona*-like infections in dogs.^{1,4-8}

Clinical signs are typically neurological, with ataxia and paraparesis. Lesions have been identified in the brain, skeletal muscle, eye, lung, liver, skin, spinal cord, heart, intestine, nasal turbinates, and tongue, with the majority of cases have lesions restricted to the muscle, brain or spinal cord.¹ Recently two species of *Sarcocystis* were named that caused myositis and hepatitis in dogs. However, there were limited availability of liver tissue in this study and the specific etiology of hepatitis was not identified. The authors suggest that schizogonic multiplication may have caused the hepatitis prior to the sarcocyst development that led to the myositis.³

Sarcocystis- associated hepatitis has been reported in many species including dogs, however this is usually due to *S. canis*.⁹

This appears to be a case of systemic *S. neurona* infection in a young adult bloodhound. Susceptibility to infection may have been increased by chronic administration of immunosuppressive drugs to treat allergies and suspect sterile meningitis. While it is possible that this dog's earlier neurologic signs were due to *S. neurona* infection of the CNS, the brain and spinal cord unfortunately were not available for histologic examination. As opposed to previous reports of *S. neurona* infection in dogs, which describe scattered organisms and limited inflammation,⁵ the lung and liver in this dog contained large numbers of merozoites and schizonts with severe associated inflammation and necrosis, which could be related to treatment with immunosuppressive drugs.

Acknowledgements

We would like to thank the following individuals for their assistance in the work-up and presentation of this case:

Dr. Charles Bailey, DVM, DACVP
Dr. Sarah Poynton, PhD
Dr. Sarah Beck, DVM, PhD, DACVP
Dr. Joseph Mankowski, DVM, PhD, DACVP
Ms. Patricia Wilcox
Ms. Jan Shivers

References:

1. Dubey JP, Howe DK, Furr M, et al. An update on *Sarcocystis neurona* infections in animals and equine protozoal myeloencephalitis (EPM). *Vet Parasitol.* 2015;209(1-2):1-42. doi:10.1016/j.vetpar.2015.01.026
2. Dubey, J.P., Calero-Bernal, R., Rosenthal, B.M., Speer, C.S., Fayer R. *Sarcocystosis of Animals and Humans, Second Edition.* Second. CRC Press; 2015.
3. Dubey JP, Sykes JE, Shelton GD, et al. *Sarcocystis caninum* and *Sarcocystis svanaei* n. spp. (Apicomplexa: Sarcocystidae) associated with severe myositis and hepatitis in the domestic dog (*Canis familiaris*). *J Eukaryot Microbiol.* 2015;62(3):307-317. doi:10.1111/jeu.12182
4. Gerhold R, Newman SJ, Grunewald CM, Crews A, Hodshon A, Su C. Acute onset of encephalomyelitis with atypical lesions associated with dual infection of *Sarcocystis neurona* and *Toxoplasma gondii* in a dog. *Vet Parasitol.* 2014;205(3-4):697-701. doi:10.1016/j.vetpar.2014.09.008
5. Dubey JP, Black SS, Verma SK, et al. *Sarcocystis neurona* schizonts-associated encephalitis, chorioretinitis, and myositis in a two-month-old dog simulating toxoplasmosis, and presence of mature sarcocysts in muscles. *Vet Parasitol.* 2014;202(3-4):194-200. doi:10.1016/j.vetpar.2014.02.055
6. Vashisht K, Lichtensteiger CA, Miller LA, Gondim LFP, McAllister MM. Naturally occurring *Sarcocystis neurona*-like infection in a dog with myositis. *Vet Parasitol.* 2005;133(1):19-25. doi:10.1016/j.vetpar.2005.04.042
7. Dubey JP, Chapman JL, Rosenthal BM, Mense M, Schueler RL. Clinical *Sarcocystis neurona*, *Sarcocystis canis*, *Toxoplasma gondii*, and *Neospora caninum* infections in dogs. *Vet Parasitol.* 2006;137(1-2):36-49. doi:10.1016/j.vetpar.2005.12.017
8. Cooley AJ, Barr B, Rejmanek D. *Sarcocystis neurona* encephalitis in a dog. *Vet Pathol.* 2007;44(6):956-961. doi:10.1354/vp.44-6-956
9. Allison R, Williams P, Lansdowne J, Lappin M, Jensen T, Lindsay D. Fatal hepatic sarcocystosis in a puppy with eosinophilia and eosinophilic peritoneal effusion. *Vet Clin Pathol.* 2006;35(3):353-357. doi:10.1111/j.1939-165X.2006.tb00148.x

NEVPC Case #8

CONTRIBUTOR(S):

Ileana Miranda, DVM, MS; April Choi, DVM, PhD, DACVP; Teresa Southard, DVM, PhD, DACVP

INSTITUTION:

Cornell University, College of Veterinary Medicine, Department of Biomedical Sciences, Section of Anatomic Pathology

SIGNALMENT:

9-year-old, female spayed, Pit Bull dog

HISTORY:

The animal was immunosuppressed for immune-mediated thrombocytopenia therapy.

GROSS FINDINGS:

N/A

HISTOPATHOLOGIC FINDINGS:

Liver: Multifocally throughout the section, hepatocytes are severely expanded by large, clear cytoplasmic vacuoles that peripheralize the nucleus (ballooning degeneration). Randomly, scattered clusters of hepatocytes are replaced by a mixture of an eosinophilic, fibrillar material (fibrin), erythrocytes, cellular and karyorrhectic debris, intact and degenerate neutrophils, and fewer macrophages (liquefactive necrosis). Occasionally, hepatocytes are shrunken with hypereosinophilic cytoplasm and pyknotic or karyorrhectic nuclei (coagulative necrosis). Associated with the areas of necrosis are small clusters of 4 x 2 micron basophilic zoites. The majority of the zoites are extracellular, but small numbers are within hepatocytes or macrophages. Multifocally, canaliculi are filled with yellow to orange, globular pigment (canalicular cholestasis). A similar material is in the cytoplasm of a few hepatocytes. The sinusoids are multifocally congested. The periportal, central, and subcapsular lymphatic vessels, as well as portal and central veins are multifocally dilated. Some portal tracts are expanded by mildly increased numbers of bile ducts and moderate infiltrates of neutrophils, lymphocytes, and plasma cells. The bile ducts are frequently dilated and filled with moderate amounts of a pale, amphophilic, fibrillar material (mucin), or rarely aggregates of a dense, brown to basophilic, granular material (microliths), occasionally admixed with cellular and karyorrhectic debris. Multifocally, the biliary epithelial cells exhibit intracytoplasmic vacuolization or individual cell necrosis, and these bile ducts are frequently surrounded by loose, concentric bundles of fibrous connective tissue. Small aggregates of macrophages laden with both lipid vacuoles and a variably yellow to brown pigment (hemosiderin and lipofuscin) are scattered throughout the section.

Immunohistochemistry Results:

Neospora sp: Protozoal organisms throughout the section exhibit strong immunoreactivity. Positive and negative controls are adequate.

Toxoplasma sp: No immunoreactivity is detected. Positive and negative controls are adequate.

MORPHOLOGIC/ETIOLOGIC DIAGNOSIS:

Liver: Moderate, multifocal, acute, necrosuppurative hepatitis with hepatocellular degeneration, canalicular cholestasis, and extra and intracellular zoites, etiology consistent with *Neospora caninum*

DISCUSSION:

Neospora caninum is an obligate intracellular coccidian parasite in the phylum Apicomplexa, family Sarcocystidae, which is histologically similar to, but biologically different from, *Toxoplasma gondii*. Naturally occurring neosporosis has been reported in dogs, cats, cattle, sheep, goats, deer, water buffalo, antelope, rhinoceros, and horses. However, in general, neosporosis is primarily considered a disease of cattle and dogs and is not zoonotic, whereas toxoplasmosis can infect humans and a wide variety of other animals.⁶ Domestic and wild canids are the only known definitive hosts for *N. caninum*, and they can also serve as intermediate hosts. The disease is acquired through ingestion of infected tissues or transplacentally from infected dams.⁵

Young dogs and puppies infected in utero typically develop lesions in the skeletal muscles and spinal nerve roots causing ascending paralysis, which tends to be most severe in the hind limbs.⁶ In adult dogs, the disease may be localized or generalized, and virtually any organ may be involved. Clinical signs vary depending on the degree of tissue invasion and the amount of cellular necrosis caused by the pathogen's intracellular replication (tachyzoite stage).² Subclinical neosporosis occurs when the parasites localize as tissue cysts containing bradyzoites; the cysts can persist within the tissue and may reserve the potential for reactivation later in life.^{2,4} The most common sites for tissue cyst localization are the central nervous system and muscle.^{1,3} Widespread involvement of the CNS and other organs (heart, liver, lungs, skeletal muscle, skin, and liver) occurs in adult dogs with disseminated disease.⁶

Clinical manifestation of neosporosis in dogs is commonly associated with immunosuppression. Studies on dogs infected with *N. caninum* and receiving corticosteroid therapy have demonstrated that these animals shed more oocysts than immunocompetent animals.^{5,10} Similar to the present case, hepatic neosporosis has been diagnosed in two adult dogs following drug-induced immunosuppression for immune-mediated hemolytic anemia⁷ and pemphigus foliaceus.⁸ Hepatitis was also the most prominent feature in an 8-month-old dog diagnosed with widely disseminated *Neospora* sp. infection, without association with immunosuppressive treatment, suggesting an alternate pathogenesis than exogenous immunosuppression.³

In this case, the extent of liver involvement is uncertain because only fragments of tissue collected post-mortem were submitted to our diagnostic laboratory, without a detailed clinical history. It is also unknown whether the current case occurred due to reactivation of congenital infection or recent acquisition. As clinical and experimental evidence has shown recrudescence of latent *N. caninum* with the administration of glucocorticoids,^{4,7} we speculate that the use of immunosuppressive therapy in this patient contributed to the activation and clinical manifestation of disease.

REFERENCES:

1. Barber JS, Trees AJ. Naturally occurring vertical transmission of *Neospora caninum* in dogs. *Int J Parasitol.* 1998;28:57–64.

2. Buxton D, McAllister MM, Dubey JP. The comparative pathogenesis of neosporosis. *Trends Parasitol.* 2002;18:546–552.
3. Dubey JP, Carpenter JL, Speer CA, Topper MJ, Uggla A. Newly recognized fatal protozoan disease of dogs. *J Am Vet Med Assoc.* 1988;192:1269–1285.
4. Dubey JP, Koestner A, Piper RC. Repeated transplacental transmission of *Neospora caninum* in dogs. *J Am Vet Med Assoc.* 1990;197:857–860.
5. Dubey JP, Schares G, Ortega-Mora LM. Epidemiology and control of neosporosis and *Neospora caninum*. *Clin Microbiol Rev.* 2007;20:323–367.
6. Dubey JP, Schares G. Neosporosis in animals – the last five years. *Vet Parasitol.* 2011;180:90–108.
7. Fry DR, McSporran KD, Ellis JT, Harvey C. Protozoal hepatitis associated with immunosuppressive therapy in a dog. *J Vet Intern Med.* 2009;23:366–368.
8. Hoon-Hanks LL, Regan D, Dubey JP, Carol Porter M, Duncan CG. Hepatic neosporosis in a dog treated for pemphigus foliaceus. *J Vet Diagn Invest.* 2013;25:807–810.
9. 2013;25:807–810.
10. Lindsay DS, Ritter DM, Brake D. Oocyst excretion in dogs fed mouse brains containing tissue cysts of a cloned line of *Neospora caninum*. *J Parasitol.* 2001;87:909–911.

ACKNOWLEDGMENTS:

I would like to thank Dr. Alina Demeter for sharing this interesting case, and our histology laboratory staff for the slide preparation.

C.L. Davis 2018

Northeastern Veterinary Pathology Conference

NEVPC Case 21

CONTRIBUTOR(S)/INSTITUTION:

David Rotstein, DVM, MPVM, DACVP
Marine Mammal Pathology Services
Olney, MD

Denise M. Boyd Hada M. Herring, M.P.S., Daniel A. Levine, Molly R. Schubert, Jess Blackburn
Kara Noonan
Florida Marine Mammal Stranding Network: Florida Wildlife Commission
St. Petersburg, FL

Slide #: 17PL-053

SIGNALMENT:

A 271.0 cm, male Atlantic bottlenose dolphin (*Tursiops truncatus*).

HISTORY:

The dolphin stranded dead on the west coast of Florida. There was no prior history of observation of this dolphin. The dolphin was recovered near dredge operations.

GROSS FINDINGS:

The dolphin was in thin body condition. There was hemorrhage in the soft tissue along the left mandible, dorsal head, and cranial aspect of the left scapula. On the head and right maxilla, there were coalescing, raised, irregular gray brown masses with ulcerative foci. The lungs were heavy and dense; blood exudated on cut surface. The diaphragm was focally fibrotic with corresponding fibrosis of the left parietal pleura and lung. A stringray barb was embedded in the liver. The gastrointestinal tract was empty. Low levels of brevetoxin (Br) and domoic acid (DA) were found in the kidney (Br-<LD, DA-4.2 ng/g), liver (Br-9.1 ng/g, DA-5.4 ng/g), stomach (Br-62.7, DA-<LD), and urine (Br-0.8 ng/ml, DA-0.4 ng/ml).

HISTOPATHOLOGIC/CYTOLOGIC FINDINGS:

Two sections of the right maxilla and head are examined. In one section, there is a wedge-shaped ulceration of the epidermis. Flanking epidermis is moderately hyperplastic. Within the ulcerated sites, there is a granulomatous infiltrate which effaces the dermis. Granulomas are composed of several multinucleated giant cells, macrophages, lymphocytes, plasma cells, clusters of degenerate neutrophils, and necrotic cellular debris. Within macrophages and multinucleated giant cells, there are 5 to 7 µm yeast-like organisms which are pale eosinophilic. Organisms are present in chains, clusters, or are connected to adjacent yeast by a thin neck. In the second section, there is moderate epithelial hyperplasia. The dermis is expanded by mature collagen and streaming fibroblasts.

MORPHOLOGIC/ETIOLOGIC DIAGNOSIS:

Skin: Dermatitis, ulcerative and granulomatous, chronic-active, marked with intralesional fungal yeast. (Etiology: *Paracoccidioides* spp.; formerly *Lacazia loboi*).

DISCUSSION:

The cause of stranding was attributed to peracute drowning. Both brevetoxin and domoic acid could have played a role. The fungal dermatitis is an incidental observation and has been observed in *T. truncatus* from the east and west coast of Florida and rarely from North Carolina (Rotstein et al., 2009). Prevalence rates in nearby Sarasota Bay and Charlotte Harbor were 2% for both regions (Burdett-Hart et al., 2011). Infection in people in South America has also been reported. Infection is nearly always epithelial though regional lymph node involvement has been rarely reported (Opromolla et al., 2003).

The observation of fungal infection has been separated into definitive diagnosis with histopathology (lacaziosis) and suspected based on photographic observations (lacaziosis-like diseases). The organism has never been cultivated. The nomenclature is confusing and has gone through several different scientific names, most recently *Loboa lobo* and *Lacazia lobo*. Recent molecular diagnostics have changed the nomenclature with cases previously attributed to *Lacazia lobo* actually being *Paracoccidioides* spp (Viela et al., 2016).

REFERENCES:

Burdett Hart L, Rotstein DS, Wells RS, Bassos-Hull K, Schwacke LH. 2011. Lacasiosis and lacaziosis-like prevalence among wild, common bottlenose dolphins *Tursiops truncatus* from the west coast of Florida, USA. *Dis Aquat Organ* 95: 49-56.

Opromolla DV, Belone AF, Tabroda PR, Rosa PS. 2003. Lymph node involvement in Jorge Lobo's disease: Report of two cases. *Int J Dermatol* 42: 938-941.

Rotstein DS, Burdett LG, McLellan W, Schwacke L, Rowles T, Terio KA, Schultz S, Pabst A. Lobomyocosis in offshore bottlenose dolphins (*Tursiops truncatus*), North Carolina. *Emerg Infect Dis* 15: 588-590.

Vilela R, Bossart GD, St. Leger JA, Dalton LM, Reif JS, Schaefer AM, McCarth PJ, Fair PA, Mendoza L. 2016. Cutaneous granulomas in dolphin caused by novel uncultivated *Paracoccidioides brasiliensis*. *Emerg Infect Dis* 22: 2063-2069.

ACKNOWLEDGMENTS:

University of Florida Histopathology Lab

NEVPC Case 10

CONTRIBUTOR(S)/INSTITUTION:

Alina Elena Demeter DMV, PhD; April Choi, DVM, PhD, DACVP; Andrew Miller DVM, DACVP

Cornell University Department of Biomedical Sciences; Section of Anatomic Pathology

SIGNALMENT: 10-year-old, male castrated, domestic short hair cat

HISTORY:

Common bile duct and liver punch biopsies were submitted for this patient. The patient had a history of increased liver enzymes, decreased appetite, mild to moderate weight loss and lethargy, and more recently, jaundice.

CBC/Chemistry values provided: ALT: 246 U/L (12-133), total bilirubin: 3.4 mg/dL (0-0.9); GGT: 23 U/L (0-4); ALP: 89 U/L (14-111); Hct: 24.8 %; leukocytosis (20.39 K/uL); neutrophilia (18.2 K/uL); PTT: 99.8; PT: 16.9.

Variable increases of ALP and GGT (specific values not available) were reported in the past 2 months. Ultrasound revealed a mildly enlarged, hyperechoic liver with a significantly dilated common bile duct. Irregular echogenic material was reported in the common bile duct and gall bladder. The patient had an exploratory laparotomy with placement of biliary stent and removal of the common bile duct material.

GROSS FINDINGS: None reported.

HISTOPATHOLOGIC/CYTOLOGIC FINDINGS:

Common bile duct (slide 1): The sections are characterized by an invasive, non-encapsulated, hypercellular neoplasm, composed of islands, poorly defined tubules, and nests of neoplastic cells, supported by a delicate fibrovascular stroma. The neoplastic cells have organized nuclear polarity, are predominantly polygonal, with indistinct cell borders and a moderate amount of pale eosinophilic, slightly fibrillar cytoplasm. The nuclei are predominantly oval with finely stippled chromatin and punctate nucleoli. Anisocytosis and anisokaryosis are mild. There are rare karyomegalic cells and 13 mitotic figures in ten 400 X fields. In multiple areas, the neoplasm is margined by a loosely arranged, pale eosinophilic, hypocellular stroma, infiltrated with abundant neutrophils, macrophages, hemosiderin-laden macrophages and fewer lymphocytes and plasma cells. Multiple islands of neoplastic cells are noted away from the main masses. Within the lamina propria are frequent aggregates of an intensely eosinophilic, fibrillar, hypocellular material (fibrin), and abundant hemorrhage. The neoplastic cells reach all surgical margins.

Liver (slide 2): Overall the liver architecture is distorted by a nodular appearance of individual liver lobules. Increased numbers of bile ducts extend from the portal tracts, and uniting portal tracts with one another. The portal tracts are characterized by multiple bile duct profiles, of variable diameters, frequently enclosed within a few layers of fibrous tissue that is occasionally onion skin-like (peribiliary edema and fibrosis). Along with the abundant small caliber bile ducts are poorly defined hepatic progenitor cells and hemosiderin-laden macrophages as well as occasional lipogranulomas, characterized by lipid-laden macrophages. A small number of lymphocytes and plasma cells are within the portal tracts (mild cholangitis), that do not extend beyond the limiting plate and rarely surrounding the central veins. The expanded portal tracts are infiltrated by scattered plasma cells and lymphocytes and enclosed within a few layers of fibrous tissue along with mature collagen. Within the remaining

parenchyma, in the centrilobular areas, the hepatocytes contain abundant lipofuscin pigment in the cytoplasm. There is a moderate number of Kupffer cells throughout the parenchyma (hypertrophy) and rare individual hepatocellular necrosis. Also within the expanded portal tracts there are globular aggregates of an intensely eosinophilic to pale eosinophilic, amorphous, waxy, acellular material within macrophages (mucin). No neoplasia is noted.

HISTOCHEMICAL AND IMMUNOHISTOCHEMICAL STAINS:

An immunohistochemical stain for identification of cells of neuroendocrine origin (Chromogranin A) of sections of bile duct (slide 1) reveals intermediate to strong intracytoplasmic, granular immunoreactivity in approximately 70% of the neoplastic cells.

Two immunohistochemical stains for the identification of cells of epithelial origin (CK AE1/AE3) and hepatocytes (Hep Par 1) of sections of bile duct (slide 1) have no immunoreactivity in the neoplastic cells.

An immunohistochemical stain for identification of mitotic activity (Ki67) of sections of liver (slide 2) reveals multifocal, strong nuclear immunoreactivity within small bile ducts (ductular reaction).

An immunohistochemical stain for identification of biliary epithelial cells expressing cytokeratin 19 (CK19) of sections of liver (slide 2) reveals multifocal immunoreactivity restricted to the cytoplasm of cells within the ductular reaction.

In all cases, the positive and negative controls have appropriate immunoreactivity.

Two histochemical stains to better characterize liver architecture (reticulin) and fibrosis (Masson's trichrome) of sections of liver (slide 2) were assessed: The stains highlight the expansion of the portal tracts, sending thin tendrils of reticulin and collagen, uniting the portal tracts with one another and highlighting the liver lobules. The trichrome stain reveals loosely arranged (edematous) collagen in multiple areas, encircling the bile ducts (peribiliary fibrosis) and bridging portal to portal fibrosis. A histochemical stain for identification of amyloid (Congo red) of sections of liver (slide 2) does not reveal any amyloid.

MORPHOLOGIC/ETIOLOGIC DIAGNOSIS:

Liver:

1. Marked, multifocal to coalescing, portal and periportal ductular reaction
2. Mild, multifocal, subacute, lymphoplasmacytic cholangitis with moderate peribiliary edema and fibrosis

Common bile duct: Neuroendocrine carcinoma

DISCUSSION:

Histopathology examination of the common bile duct mass reveals a neuroendocrine carcinoma (carcinoid), a diagnosis confirmed by the positive chromogranin A stain.

Carcinoids are considered rare tumors in domestic species originating from the diffuse neuroendocrine population distributed throughout the biliary epithelium¹. Reports of feline hepatic carcinoids are rare, with the first reported case in 1992². In cats, carcinoids more frequently originate from the intra and extrahepatic biliary tree. In a study of 17 cats with hepatobiliary neuroendocrine carcinoma, nine were extrahepatic and the median age of the patients was nine years old³, similar with this case. In case of intrahepatic biliary tree carcinoids, frequently multiple liver lobes are affected. The extrahepatic carcinoids generally do not metastasize into the liver. Liver enzymes are typically more elevated in cats with extrahepatic carcinoids than those with intrahepatic carcinoids.

While the common bile duct neoplasm did not pose a diagnostic dilemma, the liver findings, particularly regarding the bile duct proliferation were more challenging to interpret. The presence of an obvious cause for bile duct obstruction along with peribiliary edema and fibrosis support a ductular reaction (type I); however, there is considerable overlap between ductular reactions (DR) and ductal plate malformations. Four types of ductular reactions are characterized and recognized in human hepatopathology: type I, proliferation of previously existing ducts and ductules, type IIA, characterized by periportal ductular metaplasia of hepatocytes, type IIB, pericentral ductular metaplasia of mature hepatocytes associated with myofibroblast induced fibrosis and type III, proliferation of liver stem progenitor cells in ductules and canals of Hering^{4,5,6}. Type I DR is predominant in complete bile duct obstructions, cytokine-induced ductular increase (in inflammatory diseases of the biliary tree) and alpha-naphthyl isothiocyanate intoxication⁴. Ductal plate malformation refers to improper or arrested modeling of the ductal plate during embryogenesis and is often associated with abnormalities of development of the portal veins, reflecting the intimate association of the vascular system and the mesenchyme during development of the portal tracts⁷. In this case, the portal veins were identified in most examined portal tracts, and evaluated to be within normal limits. The malformed ducts are highly susceptible to bacterial colonization, hence patients with ductal plate malformation are usually diagnosed when developing cholangitis/cholangiohepatitis⁷.

Type I and IIA ductular reactions are reversible⁴ and to our knowledge this is the only way to prove that the liver changes are indeed type I DR; re-biopsy of the liver once the clinical signs have subsided and the liver enzyme level is normalized.

REFERENCES:

1. Kazuyoshi N, Masazumi T, Hideaki N, Hitoshi I: Composite glandular-endocrine cell carcinoma of the extra-hepatic bile duct: immunohistochemical study. *Pathology* 25: 90–94, 1993
2. Patnaik AK: A morphologic and immunocytochemical study of hepatic neoplasms in cats. *Vet Pathol* 29: 405–415, 1992
3. Patnaik, A.K., Lieberman, P.H., et al., Hepatobiliary neuroendocrine carcinoma in cats: a clinicopathologic, immunohistochemical, and ultrastructural study of 17 cases. *Vet Pathol* 42:331–337.
4. Desmet J. Valler, Ductal plates in hepatic ductular reactions. Hypothesis and implications. I. Types of ductular reaction reconsidered. *Virchows Arch*, 458:251–259, 2011
5. Desmet J. Valler, Ductal plates in hepatic ductular reactions. Hypothesis and implications. II. Ontogenic liver growth in childhood. *Virchows Arch*, 458:261–270, 2011
6. Desmet J. Valler, Ductal plates in hepatic ductular reactions. Hypothesis and implications. III. Implications for liver pathology. *Virchows Arch*, 458:271–279, 2011
7. S. Pillai et al., Ductal plate malformation in the liver of boxer dogs: Clinical and histological features, *Veterinary Pathology*, Volume: 53, issue: 3, page(s): 602-613, 2016

ACKNOWLEDGMENTS:

Thank you to Dr. Sean P. McDonough and Dr. Sharon Center, for their keen explanations and insight into ductal plate malformation and ductular reactions and to the referring veterinarian, Dr. Krysta Deitz for the excellent history provided.

2018 Northeastern Veterinary Pathology Conference – Joint Pathology Center April 7-8

Case Submission Form

NEVPC CASE # 11

IDENTIFICATION NUMBER ON SOURCE MATERIAL: 1658-18, Cornell University

CONTRIBUTOR(S)/INSTITUTION: Timothy Wu, MS, DVM¹; Katie Kelly DVM, PhD, DACVP¹; April Choi, DVM, PhD¹; Sharon A. Center DVM, DACVIM²

¹Cornell University, College of Veterinary Medicine, Department of Biomedical Sciences, Section of Anatomic Pathology

²Cornell University, College of Veterinary Medicine, Department of Clinical Sciences

SIGNALMENT: 10 year-old, female spayed, Scottish Terrier dog

HISTORY:

A 10-year-old, female spayed Scottish Terrier dog presented for evaluation of a cavitated liver mass. The patient had historically elevated ALP and ALT levels of 3 years duration, with more recent increases in enzyme activity.

Abdominal ultrasound revealed diffuse mottling throughout the liver and a large, approximately 7 x 7 x 4 cm, focal, cavitated liver mass in the left lateral liver lobe. Multiple renal cortical cysts and splenic nodules were also detected. Previous ultrasound examinations reported a normal appearing urinary bladder; there is a history of urinary bladder neoplasia among littermates.

Thoracic and abdominal CT imaging was performed, revealing a large mass in the left lateral liver lobe, with a second smaller mass within the caudate liver lobe, and multiple ill-defined small densities within the lungs. The patient was taken to surgery, where the masses on the left lateral and caudate liver lobes were removed by a partial liver lobectomy, and additional biopsies of the left and right medial lobes were also taken for histopathology. The patient recovered uneventfully and was discharged 2 days following the surgery.

GROSS FINDINGS:

At the time of surgery, an approximately 10 cm diameter mass was noted on the caudal edge of the left lateral liver lobe. A smaller, approximately 5 cm diameter mass was present on the distal end of the caudate liver lobe. No additional abnormalities were reported.

HISTOPATHOLOGIC/CYTOLOGIC FINDINGS:

Left lateral liver lobe: Effacing and replacing the hepatic parenchyma is a large, expansile, multilobular, unencapsulated, variably cystic mass composed of polygonal cells arranged in haphazard anastomosing cords up to 6 cells wide, within a moderate fibrovascular stroma (hepatocellular tumor) Neoplastic hepatocytes have distinct cell borders, with a moderate amount of granular, eosinophilic cytoplasm, and round to oval, central nuclei with finely stippled chromatin and a single prominent nucleolus. Neoplastic hepatocytes exhibit mild anisocytosis and anisokaryosis, with occasional binucleated cells. Mitoses are 1 in ten 400X high powered fields. Multifocally, neoplastic cells surround large cystic structures containing clear space, filled with free erythrocytes, hemosiderin-laden macrophages, vacuolated hepatocytes, fibrous connective tissue, and large tubular structures lined by a single layer of tall columnar epithelial cells with abundant, vacuolated, eosinophilic cytoplasm, and round, basal nuclei with finely stippled chromatin and a single prominent nucleolus (reactive biliary epithelium).

Multifocally associated with cystic areas are a second population of neoplastic epithelial cells arranged in islands and broad trabeculae, with variably distinct cell borders, a moderate amount of pale eosinophilic cytoplasm, and central, round to oval nuclei with finely stippled chromatin and occasional nucleoli. Cells exhibit mild anisocytosis and anisokaryosis. Mitoses are 1 in ten 400X high powered fields. In the parenchyma adjacent to the tumors, hepatocytes contain a moderate amount of intracytoplasmic,

irregular, clear vacuoles (glycogen-type vacuolar hepatopathy), and sharply demarcated, clear, lipid vacuoles, which peripheralize the nucleus (macrovesicular lipidosis). The bile ducts are dilated multifocally.

The following immunohistochemical stains are applied:

HEPPAR1 stain for hepatocytes: The examined section of mass is composed of two populations of neoplastic cells. The first population has poorly organized cords of hepatocytes, while the second population consists of multifocal cystic areas lined by lobules of polygonal neoplastic cells. There is a sharp demarcation in immunoreactivity, in which all of the neoplastic hepatocytes exhibit strong membranous and intracytoplasmic immunoreactivity (internal positive control), while the lobular population of neoplastic cells adjacent to the cystic structures are diffusely non-reactive.

Cytokeratin 19 (CK19) stain for epithelial cells, including biliary and urinary epithelium: Approximately 80% of lobules of cells adjacent to cystic areas exhibit strong membranous and intracytoplasmic immunoreactivity.

Cytokeratin 7 (CK7) stain for epithelial cells, including biliary and urinary epithelium: Approximately 10% of lobules of cells adjacent to cystic areas exhibit strong membranous and intracytoplasmic immunoreactivity.

Uroplakin III (UPIII) stain for urothelium: There is moderate background staining and brown pigment (hemosiderin and lipofuscin) within macrophages. No neoplastic cells exhibit immunoreactivity.

Cytokeratin 20 (CK20) stain for epithelial cells, including biliary and urinary epithelium: No neoplastic cells exhibit immunoreactivity.

Positive and negative controls are adequate for all examined sections

MORPHOLOGIC/ETIOLOGIC DIAGNOSIS:

Liver:

1. Hepatocellular carcinoma, trabecular type, with intratumoral metastatic carcinoma
2. Mild, multifocal, nondegenerative glycogen-type vacuolar hepatopathy
3. Mild, multifocal macrovesicular hepatic lipidosis

DISCUSSION:

Histologic evaluation reveals a hepatocellular carcinoma containing apparent intratumoral metastasis with adjacent mild hepatic lipidosis and diffuse non-degenerative glycogen-type vacuolar hepatopathy within the left lateral liver lobe. Additional examined sections revealed hepatocellular carcinoma within the caudate lobe, though no intratumoral metastases were noted these sections. Vacuolar hepatopathy (VH) is a common syndrome in dogs, usually reflecting hepatocellular cytosolic glycogen accumulation, observed histologically as swollen hepatocytes with clear and wispy cytoplasm, which stains positive with PAS.⁽¹⁾ VH is typically associated with iatrogenic administration or endogenous overproduction of glucocorticoids, though inflammatory, neoplastic, and infectious disorders may also cause VH.⁽²⁾

Scottish Terriers are known to develop progressive vacuolar hepatopathy with elevated alkaline phosphatase (ALP) activity.^(1, 3) In a retrospective study, examination of 97 Scottish Terrier liver biopsies revealed that approximately 70% of biopsies had marked vacuolar hepatopathy.⁽⁴⁾ Multiple etiologies have been posited for this breed predisposition, including non-clinical hyperadrenocorticism,⁽⁵⁾ neoplasia, hepatobiliary disease, physiologic stress⁽²⁾, and genetic mutation.⁽⁴⁾

It has been noted that progressive VH leads to diffuse hepatic remodeling, as vacuolated hepatocytes undergo individual hepatocyte necrosis, with subsequent hepatic cord remodeling and formation of parenchymal nodules.⁽⁶⁾ Associations have also been made between VH, hepatic fibrosis, and hepatocellular carcinoma (HCC).⁽¹⁾ In a recent study, it was found that 39 of 114 (34%) of Scottish Terriers with vacuolar hepatopathy had HCC detected at surgery or necropsy, or via abdominal

ultrasonography.⁽⁶⁾ Histologic findings in this study suggested that HCC was seemingly preceded by dysplastic hepatocellular foci (which were noted in other examined sections of liver from this patient).⁽⁶⁾ The study also found increased sex hormone concentrations (progesterone and androstenedione), supporting adrenal gland hyperactivity in 88% of dogs tested.⁽⁶⁾ From these results, it was postulated that an inherited genetic disorder affects adrenal steroidogenesis, with subsequent ALP induction, hepatocellular glycogen accumulation, progressive VH, and ultimate formation of HCC.⁽⁶⁾

Hepatocellular carcinoma is the most common primary hepatobiliary neoplasm in the dog where it is often a solitary lesion but also may be multifocal and less commonly metastatic. Diagnosis is often initiated because of prominent increases in alkaline phosphatase (ALP) or asymmetric hepatomegaly, pursued with ultrasound imaging that discovers of an intrahepatic mass lesion. However, this neoplasm is also serendipitously recognized during abdominal ultrasound or exploratory laparotomy initiated for some other health concerns. Clinical discovery of metastatic HCC is relatively uncommon. Published rates of metastasis are discordant, ranging from less than 25% to 61%, when present metastatic spread typically involves regional lymph nodes, lung, and peritoneum.^(7, 8) HCC was reported with a frequency of 0.46% in a retrospective study of 12,245 canine necropsies.⁽⁸⁾ However, of the 446 cases of HCC in over 33 years at Cornell University Hospital for Animals, 5% of these cases were Scottish Terriers, representing a 10-fold relative risk for HCC development in this breed.⁽⁶⁾

This case is unique in that the hepatocellular carcinoma contains a distinct separate population of neoplastic cells. These cells display histologic characteristics consistent with a carcinoma (formation of islands and trabeculae) different than the surrounding HCC. Characterization via immunohistochemistry reveals that these neoplastic cells are CK19++ +/-CK7+/HEPPAR1-/CK20-/UPIII- and distinct from the immunoreactivity of HCC cells. Collision tumor or cholangiocellular transformation of neoplastic cells was considered. We considered the sharp demarcation between HEPPAR1 positive cells and CK19 positive cells more consistent with a metastatic event rather than a graduation transformation of neoplastic cells. Although the cells are immunoreactive for CK19, with weaker immunoreactivity for CK7, the overall pattern (lack of acini and tubule formation) is not typical for cholangiocellular carcinoma. We also considered hepatic carcinoids. However, the age of the animal, and the lack of associated histologic features, including formation of rosettes and ribbons, cells with granular cytoplasm, frequent mitoses, and abundant fibrosis decreased the likelihood of this differential.⁽⁹⁾

Considering the breed of the patient, and the history of bladder neoplasia in littermates, a metastatic transitional cell (urothelial) carcinoma (TCC) was considered. Knapp et al. determined that the risk of canine TCC is higher in Scottish Terriers, with a 19-fold increased risk compared with mixed breeds.⁽¹⁰⁾ Additional risk factors for TCC include female sex, history of spay or neuter, and obesity.⁽¹¹⁾ Studies have linked TCC in Scottish Terriers to environmental risks, such as exposure to lawn chemicals.⁽¹²⁾ Association with exposure to topical flea and tick pesticides was investigated as well; however, no increased risk was suggested in this study, though older products could not be evaluated due to the low sample size in this case.⁽¹³⁾ In a separate study, consumption of green leafy vegetable was found to decrease the risk of developing TCC in Scottish Terriers.⁽¹⁴⁾ Hepatic metastasis of TCC to the liver has been reported in 7% of dogs undergoing necropsy; however, this pattern of intratumoral metastasis is unusual.⁽¹¹⁾

The neoplastic cells were not immunoreactive for CK20 or UPIII; however, CK20 is restricted to superficial and occasional intermediate cells of the bladder urothelium, with only 46% of primary and metastatic tumors exhibiting positive immunoreactivity in one human study.⁽¹⁵⁾ Additionally, the lack of uroplakin III expression does not necessarily rule out a TCC. In a recent study of 99 canine proliferative urothelial lesions of the urinary bladder, it was noted that 42% of grade 3 urothelial carcinomas exhibited loss of UPIII expression.⁽¹⁶⁾ It was also reported that the majority (71%) of urothelial carcinomas exhibited a patchy CK7 immunostaining pattern, with a minority of cases losing CK7 expression. Transitional cell carcinomas have also been reported to exhibit CK19 expression, further supporting the suspicion for a TCC in this case.^(17, 18)

A recent study identified a somatic mutation in the BRAF gene in 85% of sequenced canine TCCs.⁽¹⁹⁾ BRAF mutations potentially stimulate the mitogen activated protein kinase (MAPK) pathway, leading to

constitutive cell signaling, growth factor independent proliferation, and anti-apoptotic signaling.⁽¹⁹⁾ Using this information, analysis of urine for DNA containing the BRAF mutation has been developed, with a sensitivity of 85% reported.⁽²⁰⁾ Given the histologic findings, urine from this patient has been submitted for testing, and results are pending.

REFERENCES:

1. Peyron C, Lecoindre P, Chevallier M, Guerret S, Pagnon A: Vacuolar hepatopathy in 43 French Scottish Terriers: a morphological study. *Revue Méd Vét* **166**: 7-8, 2015
2. Sepesy LM, Center SA, Randolph JF, Warner KL, Erb HN: Vacuolar hepatopathy in dogs: 336 cases (1993–2005). *Journal of the American Veterinary Medical Association* **229**: 246-252, 2006
3. Gallagher AE, Panciera DL, Panciera RJ: Hyperphosphatasemia in Scottish terriers: 7 cases. *Journal of veterinary internal medicine* **20**: 418-421, 2006
4. Center S. Breed specific hepatopathies: Scottish Terrier & Maltese dogs. *Proceedings 2012*
5. Zimmerman KL, Panciera DL, Panciera RJ, Oliver JW, Hoffmann WE, Binder EM, Randall DC, Kinnarney JH: Hyperphosphatasemia and concurrent adrenal gland dysfunction in apparently healthy Scottish Terriers. *Journal of the American Veterinary Medical Association* **237**: 178-186, 2010
6. Cortright CC, Center SA, Randolph JF, McDonough SP, Fecteau KA, Warner KL, Chiapella AM, Pierce RL, Graham AH, Wall LJ: Clinical features of progressive vacuolar hepatopathy in Scottish Terriers with and without hepatocellular carcinoma: 114 cases (1980–2013). *Journal of the American Veterinary Medical Association* **245**: 797-808, 2014
7. Trigo F, Thompson H, Breeze R, Nash A: The pathology of liver tumours in the dog. *Journal of comparative pathology* **92**: 21-39, 1982
8. Patnaik A, Hurvitz A, Lieberman P, Johnson G: Canine hepatocellular carcinoma. *Veterinary pathology* **18**: 427-438, 1981
9. Cullen JM: Tumors of the Liver and Gallbladder. *In: Tumors in Domestic Animals*, ed. Meuten DJ, Fifth ed., pp. 602-631. John Wiley & Sons, Inc., Iowa, USA, 2017
10. Knapp DW, Glickman NW, DeNicola DB, Bonney PL, Lin TL, Glickman LT. Naturally-occurring canine transitional cell carcinoma of the urinary bladder A relevant model of human invasive bladder cancer. *Urologic Oncology: Seminars and Original Investigations* 2000;47-59
11. Knapp DW, Ramos-Vara JA, Moore GE, Dhawan D, Bonney PL, Young KE: Urinary bladder cancer in dogs, a naturally occurring model for cancer biology and drug development. *ILAR journal* **55**: 100-118, 2014
12. Glickman LT, Raghavan M, Knapp DW, Bonney PL, Dawson MH: Herbicide exposure and the risk of transitional cell carcinoma of the urinary bladder in Scottish Terriers. *Journal of the American Veterinary Medical Association* **224**: 1290-1297, 2004
13. Raghavan M, Knapp DW, Dawson MH, Bonney PL, Glickman LT: Topical flea and tick pesticides and the risk of transitional cell carcinoma of the urinary bladder in Scottish Terriers. *Journal of the American Veterinary Medical Association* **225**: 389-394, 2004
14. Raghavan M, Knapp DW, Bonney PL, Dawson MH, Glickman LT: Evaluation of the effect of dietary vegetable consumption on reducing risk of transitional cell carcinoma of the urinary bladder in Scottish Terriers. *Journal of the American Veterinary Medical Association* **227**: 94-100, 2005
15. Jiang J, Ulbright TM, Younger C, Sanchez K, Bostwick DG, Koch MO, Eble JN, Cheng L: Cytokeratin 7 and cytokeratin 20 in primary urinary bladder carcinoma and matched lymph node metastasis. *Archives of pathology & laboratory medicine* **125**: 921-923, 2001
16. Sledge D, Patrick D, Fitzgerald S, Xie Y, Kiupel M: Differences in expression of uroplakin III, cytokeratin 7, and cyclooxygenase-2 in canine proliferative urothelial lesions of the urinary bladder. *Veterinary pathology* **52**: 74-82, 2015

17. Zhang H, Weimin Y, Zhangqun Y, Chunlian C, Xiao Y: Clinical significance of Cytokeratin 19 and Cytokeratin 20 in predicting recurrence of bladder transitional cell carcinoma. *The Chinese-German Journal of Clinical Oncology* **5**: 132-134, 2006
18. Nisman B, Barak V, Shapiro A, Golijanin D, Peretz T, Pode D: Evaluation of urine CYFRA 21-1 for the detection of primary and recurrent bladder carcinoma. *Cancer* **94**: 2914-2922, 2002
19. Decker B, Parker HG, Dhawan D, Kwon EM, Karlins E, Davis BW, Ramos-Vara JA, Bonney PL, McNiel EA, Knapp DW: Homologous mutation to human BRAF V600E is common in naturally occurring canine bladder cancer-evidence for a relevant model system and urine-based diagnostic test. *Molecular Cancer Research: molcanres*. 0689.2014, 2015
20. Mochizuki H, Shapiro SG, Breen M: Detection of BRAF mutation in urine DNA as a molecular diagnostic for canine urothelial and prostatic carcinoma. *PLoS one* **10**: e0144170, 2015

ACKNOWLEDGMENTS:

We would like to thank the clinical staff at the Cornell University Hospital for Animals for their clinical input and case submission and our staff in histology laboratory for the slide preparation.

NEVPC Case #12

CONTRIBUTOR(S)/INSTITUTION:

Sang Lee, DVM
Resident, Veterinary Pathology Services
Joint Pathology Center
Silver Spring, MD

SIGNALMENT: 8-year-old female domestic short hair cat

HISTORY:

The patient presented to the Fort Belvoir (military) Veterinary Treatment Facility in spring 2017 for six-month history of decreased appetite weight loss, jaundice. Cytological samples were promptly taken and sent to the JPC for impression. The patient had elevated ALP & ALT levels and the vaccination status unspecified. The initial working diagnosis of chronic pancreatitis with secondary hepatic lipidosis was given. The patient was treated with esophageal tube feeding, which help return the appetite. But, jaundice, weight loss, and elevated liver enzyme values were unresolved.

Gross Findings:

There were multifocal discrete nodules with reticulated coloration interspersed with more normal appearing sections of liver.

Ultrasonographic Findings:

Nodular pattern in the liver.

Histopathologic findings:

Liver: There are multifocal to coalescing areas of hepatic parenchyma with hepatic cord discohesion, dissociation of hepatocytes, and loss of normal sinusoidal architecture. Within the affected areas, hepatocytes contain one to multiple lymphocytes that are often surrounded by clear halo, with round nuclei and coarsely stippled chromatin. Multifocally there are areas of coagulative necrosis, as well as irregular ductular hyperplasia with luminal lymphocytes. There is multifocal hemorrhage and hemosiderin-laden Kupffer cells.

Morphologic Diagnosis: Liver: T-cell Lymphoma, hepatocytotropic.

DISCUSSION:

Hepatocytotropic T-cell lymphoma arises from cytotoxic $\gamma\delta$ T-cells and is characterized by "invasion of hepatic cords" by lymphocytes. Lymphocytes reside between hepatocytes or within invaginations of the hepatocyte cell membrane, though not technically within the cytoplasm proper. These histological features resemble what was previously described as "emperipolesis," an uncommon process in which a cell exists as viable cell within cytoplasm of another living cell. Lymphocytes in hepatocytotropic T-cell lymphoma lack membranous CD11d expression, unlike the lymphocytes of splenic origin, which is suggestive of primary hepatic origin.

REFERENCES:

1. Amita K, Shankar S, et al. Emperipolesis in a case of adult T cell lymphoblastic lymphoma (mediastinal type)-detected at FNAC and imprint cytology. *Online J Health Allied Scs.* 2011;10:11.

2. Fry, M, McGavin M. Bone marrow, blood cells, and the lymphatic system. In: Zachary JF, McGavin MD, eds. *Pathologic Basis of Veterinary Disease*. 5th ed. St. Louis, MO: Elsevier; 2012:698-705.
3. Humble JG, Jayne WHW, Pulvertaft RJV: Biological interaction between lymphocytes and other cells. *Br J Haematol*. 1956;2:283-294.
4. Keller S, Vernau W, et al. Hepatosplenic and hepatocytotropic T-cell lymphoma: two distinct types of lymphoma in dogs. *Vet Pathol*. 2012;50:281-290.
5. Kumar V, Abbas A, Aster J. Neoplasia. In: Kumar V, Abbas A, Aster J, eds. *Robbins and Cotran Pathologic Basis of Disease*. 9th ed. Philadelphia, PA; Saunders Elsevier; 2015: 296-297.
6. Ossent P, Stöckli RM, Pospischil A: Emperipolesis of lymphoid cells in feline hepatocytes. *Vet Pathol*. 1989;26:279-280.
7. Suzuki M, Kanae Y, et al. Emperipolesis-like invasion of neoplastic lymphocytes into hepatocytes in feline T-cell lymphoma. *J Comp Pathol*. 2011;144:312-316.
8. Valli V, Kiupel M, Bienzle D. Hematopoietic system. In: Maxie MG, 4th ed. *Jubb, Kennedy, and Palmer's Pathology of Domestic Animals*, Vol.3, 4th ed. Saunders Elsevier, Philadelphia, PA, 2016:103-104.
9. Wang E, Yeh S. et al. Depletion of β -catenin from mature hepatocytes of mice promotes expansion of hepatic progenitor cells and tumor development. *PNAS*. 2011;108:18384-18389

ACKNOWLEDGMENTS: I would like to acknowledge COL Derron Alves, DVM, DACVP; LTC Taylor Chance, DVM, DACVP; and MAJ Erin Ball, DVM, DACVP of the Joint Pathology Center for their contributions and assistance in signing out this case; Walter Reed National Military Medical Center's histology and immunohistochemical technical support staff for their outstanding support and quick turnaround time; and CPT Britany Beavis, DVM, Fort Belvoir Veterinary Treatment Facility Officer in Charge, for her correspondence on this case.

DISCLAIMER: The views expressed in this podium presentation are those of the author and do not reflect the official policy of the Department of Army, Navy, Air Force, Department of Defense, or U.S. Government.

NEVPC Case #13

CONTRIBUTOR(S)/INSTITUTION:

Jimmy Tarrant

University of Pennsylvania, School of Veterinary Medicine, Philadelphia, PA
VIB Center for the Biology of Disease and KU Leuven Center for Human Genetics, Leuven, Belgium

SIGNALMENT:

22-month-old male C57BL/6J

HISTORY:

Euthanized due to marked abdominal enlargement with dyspnea.

GROSS FINDINGS:

Ascites in the abdominal cavity. The entire left hepatic lobe and part of the median lobe were markedly enlarged by a mottled gray-brown multinodular mass measuring 1.5 x 1.5 x 1.0 cm. The lungs contained multiple brown nodules, measuring 1 to 3 mm in diameter, particularly along the lobar margins.

HISTOPATHOLOGIC/CYTOLOGIC FINDINGS:

The affected hepatic parenchyma was almost completely effaced by two distinct neoplasms. The first one was characterized by multiple coalescing hepatocellular adenomas (HCA) consisting of moderately cellular, unencapsulated, relatively well-demarcated, expansile masses, composed of well-differentiated neoplastic hepatocytes arranged in cords or thin trabeculae separated by a delicate sinusoidal vascular network. Scattered throughout the HCAs there were foci of increased atypia with higher N/C ratios, hyperchromatic nuclei, with neoplastic hepatocytes arranged in thicker trabecular (more than 3 cells in thickness) separated by irregularly distended sinusoids often forming pseudocystic spaces, with foci of coagulative necrosis. Those were interpreted as foci of progression suggesting a morphological diagnosis of trabecular type hepatocellular carcinoma (HCC) arising within a HCA. The second neoplastic entity arose within the previously described hepatocellular tumor as a multicentric process. These growths were infiltrating, unencapsulated and composed of dense palisades and perivascular pseudorosettes of poorly differentiated primitive cells, with a scant amount of cytoplasm, elongated hyperchromatic nuclei and a high mitotic rate. Scattered throughout were foci of coagulative necrosis, hemorrhage, and few foci of squamous differentiation. Morphologically, the tumor was consistent with a diagnosis of multicentric hepatoblastoma (HB). Histopathology of the pulmonary lesions revealed disseminated neoplastic aggregates multifocally plugging small and mid-sized pulmonary vessels (tumor emboli) and invading the surrounding parenchyma (tumor metastases). Pulmonary lesions recapitulated the two different neoplastic growths observed within the liver, with closely intermingled neoplastic hepatocytes and primitive, poorly differentiated neoplastic cells (interpreted as pulmonary metastases of HB arising within a HCC).

Immunohistochemistry of β -catenin revealed that neoplastic hepatocytes in both hepatic and pulmonary location had a mild to moderate membranous immunoreactivity, whereas a strong nucleocytoplasmic signal was evident in HB tumor cells.

MORPHOLOGIC/ETIOLOGIC DIAGNOSIS:

1. LIVER: hepatocellular adenoma; hepatocellular carcinoma; hepatoblastoma
2. LUNG: hepatocellular carcinoma and hepatoblastoma, metastatic and embolic, multifocal

DISCUSSION:

In the mouse, hepatoblastoma (HB) is a rare spontaneous tumor that typically occurs in aged males and in association with pre-existing hepatocellular neoplasms. Because of this association, murine HB was thought to represent a malignant progression of hepatocellular tumor cells. However, genomic profiling has revealed that murine HB is a distinct entity from hepatocellular tumors with a different transcriptome and mutational spectrum. Transcriptomic concordance of HB cells with embryonic hepatoblasts and hepatic pluripotent stem cells suggests that HB arises from a primordial hepatic precursor cell.

In humans, HB is predominantly reported as a solitary tumor in children under 3 years and is the most frequent malignant liver tumor in young children. There is an increased incidence in humans with a germline mutation in the *APC* gene. Murine and human HB share features such as predominance of males affected, typical metastasis to the lung, and mutations in *Ctnnb1* leading to constitutive activation of the Wnt/ β -catenin pathway. Given the differences in tumor biology, the relevance of murine HB as preclinical model to study human HB is uncertain. Among domestic animal species HBs are rare and most often reported in equine fetuses, neonates, occasionally young adult horses, with sporadic reports in young and adult sheep, a cat, a llama, and a dog.

Three histologic patterns of growth for HB are described. The fetal pattern contains uniform cuboidal to polygonal cells arranged in sheets to irregular plates or cords with bile canaliculi and low mitotic activity. The embryonal-type exhibits polygonal to spindle cells forming ribbons and rosettes; cells are typically smaller than the fetal type with more frequent mitoses. The macrotrabecular pattern resembles trabecular HCC. HB may contain squamous differentiation, extramedullary hematopoiesis, or mesenchymal derivatives such as osteoid. By immunohistochemistry HB are typically positive for alpha-fetoprotein, β -catenin, and cytokeratin.

As is typical for the mouse, HB in this case was found within and adjacent to HCC and HCA. Lung metastasis is the most commonly described site of metastasis for murine HB, however co-metastasis as observed in this case has not been previously described. A pathologic mechanism for the co-occurrence of these tumors in the mouse liver has not been proposed, however neoplastic transformation of hepatic precursor cells towards HB may be influenced by the HCC/HCA milieu.

REFERENCES:

1. Anna CH, Sills RC, Foley JF, Stockton PS, Ton TV, Devereux TR. Beta-catenin mutations and protein accumulation in all hepatoblastomas examined from B6C3F1 mice treated with anthraquinone or oxazepam. *Cancer Res.* 2000 Jun 1;60:2864–2868.
2. Bhusari S, Pandiri AR, Nagai H, et al. Genomic Profiling Reveals Unique Molecular Alterations in Hepatoblastomas and Adjacent Hepatocellular Carcinomas in B6C3F1 Mice. *Toxicol Pathol.* 2015 Dec 1;43:1114–1126.
3. Cairo S, Armengol C, De Reyniès A, et al. Hepatic stem-like phenotype and interplay of Wnt/beta-catenin and Myc signaling in aggressive childhood liver cancer. *Cancer Cell.* 2008 Dec 9;14:471–484.
4. Cullen JM. Tumors of the Liver and Gallbladder. In: Meuten DJ, ed. *Tumors in Domestic Animals.* John Wiley & Sons, Inc.; 2016:602–631.
5. Kim Y, Sills RC, Houle CD. Overview of the molecular biology of hepatocellular neoplasms and hepatoblastomas of the mouse liver. *Toxicol Pathol.* 2005;33:175–180.
6. Thoolen B, Maronpot RR, Harada T, et al. Proliferative and Nonproliferative Lesions of the Rat and Mouse Hepatobiliary System. *Toxicol Pathol.* 2010 Dec 1;38:5S–81S.

NEVPC Case 14

CONTRIBUTOR(S)/INSTITUTION:

Sarah Cudd, DVM
Resident, Veterinary Pathology Services
Joint Pathology Center
Silver Spring, MD

SIGNALMENT: 5-year-old female intact English bulldog

HISTORY:

The patient presented to the Norfolk (military) Veterinary Treatment Facility in April 2017 with a non-ulcerated, non-painful mass beneath right ear (approx. 4cm) of approximately 1 month duration. Cytological samples were promptly taken and sent to the JPC for impression. Based on subsequent recommendations, the patient was referred off-post for surgery (no surgical details provided).

GROSS FINDINGS:

The mass was approximately 4x4x4cm, round, firm, non-ulcerated, and haired, located beneath the right ear.

HISTOPATHOLOGIC/CYTOLOGIC FINDINGS:

Cytologic findings: Numerous clusters of epithelial cells with a moderate amount of finely vacuolated cytoplasm and fewer aggregates of spindle cells embedded in an eosinophilic matrix on a background of few foamy macrophages, segmented neutrophils, and windrowing erythrocytes. The presence of both proliferative epithelial cells (adenomatous component) and fewer spindle cells (myoepithelial component), neither of which appear aggressive may suggest a mixed (i.e. Pleomorphic) salivary gland tumor. The presence of minimal inflammation make salivary gland abscess, inflammation, infarction, and sialocele less likely.

Histopathologic findings: The submitted tissue is completely effaced by an unencapsulated, multilobulated, densely cellular neoplasm composed of two populations of neoplastic cells. There are polygonal cells forming tubules and acini on a dense collagenous stroma that often surrounds and separates lobules. Neoplastic polygonal cells multifocally have abundant pale eosinophilic to amphophilic cytoplasm with fine clear vacuoles that occasionally expand the cytoplasm and peripheralize the nucleus and tubules contain abundant inflammatory cells and mucinous debris. The second population are spindle cells which are arranged in long interlacing streams surrounding and separating aggregates of polygonal cells. There is abundant mitotic figures and single cell necrosis predominately within the spindle cell population. The key and unfortunate histologic finding was neoplastic cells that extend to surgical margins with no normal adjacent tissue to use to gauge invasiveness.

A battery of immunohistochemical, histochemical, and special stains were run. The polygonal cell population was positive for pancytokeratin and the mucinous material within the cytoplasm was PAS positive. Spindle cells were positive for vimentin, and had cytoplasmic immunoreactivity to calponin and nuclear immunoreactivity to p63, indicating myoepithelial origin. Finally, Masson's trichrome indicated the presence of dense bands of fibrous connective tissue (blue) which surrounds and separates neoplastic lobules.

MORPHOLOGIC/ETIOLOGIC DIAGNOSIS:

Impression: Fine needle aspirates (2), mass ventral to right ear: Salivary gland epithelial proliferation, with minimal neutrophilic and histiocytic inflammation.

MDx: Mass ventral to right ear (salivary gland): Mixed salivary gland neoplasm.

DISCUSSION: There was two main microscopic differentials for this patient: pleomorphic adenoma and salivary gland adenocarcinoma. Based on the current literature the differentiation between benign and malignant neoplasms requires histologic assessment of invasion. As cells in either case, benign or malignant, can have bizarre features. In this case, our lack of adjacent tissue hampered full histopathological diagnosis. In veterinary literature, the majority of malignant salivary gland neoplasms reported are adenocarcinomas with recurrence being a common feature, whereas, with pleomorphic adenomas, the most common benign salivary gland neoplasm reported in veterinary literature, complete surgical excision is often curative. In the present case, the patient had no regrowth at their 6 month recheck.

REFERENCES:

1. Chan JKC, Cheuk W. Tumors of the salivary glands. In: Fletcher CDM, ed. *Diagnostic Histopathology of Tumors*. 4th ed. Vol. 1. Philadelphia, PA: Elsevier; 2013:272-284.
2. Ellis GL, Auclair PL. Tumors of the salivary glands. In: Rosai J, Sobin LH, eds. *Atlas of Tumor Pathology*. 3rd Series. Fascicle 17. Washington D.C.: Armed Forces Institute of Pathology; 1996:39-57, 175-183.
3. Militerno G, Basso R, Marcato PS. Cytological diagnosis of mandibular salivary gland adenocarcinoma in a dog. *J. Vet. Med.* 2005; 52:514-516.
4. Munday JS, Lohr CV, Kiupel M. Tumors of the alimentary tract. In: Meuten DJ, ed. *Tumors in Domestic Animals*. 5th ed. Ames, IA: John Wiley & Sons; 2017:544.

ACKNOWLEDGMENTS: I would like to acknowledge COL Derron Alves, DVM, DACVP and MAJ Erin Ball, DVM, DACVP of the Joint Pathology Center for their contributions and assistance in signing out this case; Walter Reed National Military Medical Center's histology and immunohistochemical technical support staff for their outstanding support and quick turnaround time; and Sally Plichta, DVM, Norfolk Veterinary Treatment Facility Officer in Charge, for her correspondence on this case.

DISCLAIMER: The views expressed in this podium presentation are those of the author and do not reflect the official policy of the Department of Army, Navy, Air Force, Department of Defense, or U.S. Government.

2018 Northeastern Veterinary Pathology Conference

NEVPC CASE 15

IDENTIFICATION NUMBER ON SOURCE MATERIAL: 4087030-00

CONTRIBUTOR: Robert K. Kim, DVM

INSTITUTIONS: DOD Veterinary Pathology Residency Program, Joint Pathology Center, Silver Spring, MD

SIGNALMENT: 9-year-old female English shorthair guinea pig

HISTORY: This guinea pig presented for abdominal distention and paresis of the hind limbs. On palpation, an 8x6cm mass was identified in the left abdomen. Urine and fecal staining were also noted on the right hind leg. There was a decreased range of motion in both stifles.

GROSS FINDINGS: A solitary, firm, white to mottled tan, vascular, 8x6cm mass was removed from the left abdomen. The mass was not associated with the uterus or mesentery. On cut section there were areas of areas of pallor, hemorrhage, and variably sized aggregates of yellow, greasy substance.

HISTOPATHOLOGIC FINDINGS:

Abdominal mass, left side: A partially non-encapsulated, poorly demarcated, 8 × 6cm neoplasm is composed of multifocal aggregates of pleomorphic polygonal to spindle cells arranged in solid sheets to short, haphazard streams separated by a fine to moderate fibrovascular stroma. Neoplastic cells have variably distinct cell borders, scant to moderate amounts of eosinophilic cytoplasm with small clear vacuoles or a large vacuole that displaces the nucleus peripherally, 1-6 pleomorphic nuclei, basophilic coarsely stippled chromatin, 1-3 variably distinct nucleoli. Anisocytosis and anisokaryosis is marked and mitoses average 1-2 / 10 HPF and 3 / HPF in densely cellular areas that are frequently atypical. Multifocally, there are aggregates of lymphocytes and plasma cells with fibrin within vessels (fibrin thrombi). Scattered throughout the neoplasm are foci are areas pale eosinophilic areas that contain shrunken and pyknotic nuclei and cellular debris (necrosis).

MORPHOLOGIC/ETIOLOGIC DIAGNOSIS:

1. Abdominal mass, left side: Liposarcoma.

DISCUSSION: Liposarcomas are uncommon malignant tumors of adipose tissue in all species.^{4,6} These malignant variants of the lipoma are locally invasive and rarely metastasize.⁶ The World Health Organization further classifies liposarcomas into three histologic subtypes: well differentiated liposarcoma, pleomorphic, and myxoid.⁶ The well differentiated variant consists of mostly normal-appearing adipocytes with a single clear fat vacuole and peripheral nucleus admixed with fewer adipocytes that have round to oval nuclei and variably sized lipid droplets. The myxoid variant consists of a mixture

of spindle cells, lipocytes, and lipoblasts in a mucoid stroma that can be confirmed by an Alcian blue stain. The pleomorphic variant is identified by cells with markedly variable morphology to include large, pleomorphic multinucleated cells. Mitoses are frequent and often bizarre. In this case, the neoplasm resembles a pleomorphic liposarcoma.

To date, liposarcomas are most commonly reported in the canine.^{1,5,8} Reported breeds with a high incidence of liposarcoma are variable, but include Labrador and Golden Retrievers, Shetland Sheepdogs, and Beagles.^{1,2,6} Common sites include the subcutis of the ventral thorax, abdomen, and proximal limbs and less frequently from the fat cell precursors within bone marrow.⁶ Data about tumors in guinea pigs is relatively rare, with neoplasms from the respiratory or reproductive tract being the most common.³ Published data regarding the frequency of liposarcomas in guinea pigs is scarce. In 2013, a single case report confirmed a palpebral liposarcoma in an 18-month old guinea pig with histologic features of a well differentiated subtype.^{4,9} Further analysis of retrospective data by the authors concluded that liposarcomas in guinea pigs represented 3.11% of examined guinea pig tumors in comparison to 0.22% and 0.24% in dogs and cats, respectively. In a 2003 survey of spontaneous guinea pig tumors, liposarcoma was recognized in two out of 19 guinea pigs, with one being well differentiated and the other a myxoid variant.⁷

In this case, a liposarcoma exhibiting features of the pleomorphic subtype in a 9-year-old guinea pig is rare. Although the relative frequency of liposarcomas in guinea pigs may be higher in comparison to other domestic species, additional studies are warranted given the limitations of age and frequency of complete necropsies and/or biopsies conducted on this species.

REFERENCES:

1. Avallone G, Roccabianca P, Crippa L, Lepri E, Brunetti B, Bernardini C, Forni M, Olandese A, Sarli G. Histological Classification and Immunohistochemical Evaluation of MDM2 and CDK4 Expression in Canine Liposarcoma. *Vet Pathol.* 2016 Jul;53(4):773-80.
2. Baez JL, Hendrick MJ, Shofer FS, Goldkamp C, Sorenmo KU. Liposarcomas in dogs: 56 cases (1989-2000). *J Am Vet Med Assoc.* 2004 Mar 15;224(6):887-91.
3. Barthold SW, Griffey SM, Percy DH.: Pathology of Laboratory Rodents & Rabbits, 4th ed. Ames, IA: Blackwell Publishing Ltd; 2016:250-252.
4. Doria-Torra G, Martínez J, Domingo M, Vidaña B, Isidoro-Ayza M, Casanova MI, Vidal E. Liposarcoma in animals: literature review and case report in a domestic pig (*Sus scrofa*). *J Vet Diagn Invest.* 2015 Mar;27(2):196-202.
5. Gross TL, Ihrke PJ, Walder EJ, Affolter VK. *Skin Diseases of the Dog and Cat.* 2nd ed. Ames, IA: Blackwell; 2005: 766-777.

6. Hendrick MJ. Mesenchymal tumors of the skin and soft tissues. In: Meuten DJ, ed. *Tumors in Domestic Animals*. 5th ed. Ames, IA: Wiley Blackwell; 2017: 159.
7. Jelinek F. Spontaneous tumours in guinea pigs. *Acta Vet Brno* 2003;72:221-228.
8. Mauldin EA, Peters-Kennedy J. Integumentary system. In: Maxie MG, ed. *Jubb, Kennedy, and Palmer's Pathology of Domestic Animals*. Vol 2. 6th ed. New York, NY: Elsevier Limited; 2015:726.
9. Quinton JF, Ollivier F, Dally C. A case of a well-differentiated palpebral liposarcoma in a Guinea pig (*Cavia porcellus*). *Vet Ophthalmol*. 2013; 16:155-159.

ACKNOWLEDGEMENTS:

Dr. Erika Hoffeld

LTC Taylor B. Chance



NEVPC Case 16

Presenting Contributor: Elise E. B. LaDouceur, DVM, DACVP, Joint Pathology Center, 606 Stephen Sitter Avenue, Silver Spring, MD 20910

Additional Contributors: Lisa M. Mangus, DVM, PhD, DACVP, Johns Hopkins University, and Andrew N. Cartoceti, DVM, DACVP, Smithsonian National Zoo

Signalment: Thirty four, captive American horseshoe crabs (HSC; *Limulus polyphemus*) ranging from juvenile to several years old, most of which were male.

History: Histology slides of the hepatopancreas stained with HE were reviewed.

Gross Findings: This study was limited to histologic evaluation.

Histopathologic Findings: The most common finding was variably degraded metazoan parasites (trematodes) embedded in the interstitium and surrounded by one of the following responses: no appreciable inflammatory response, hemocytes, a thin fibrous rim, agranular hemocyte coagula, or combined granular/agranular hemocyte coagula. The second most common finding was decreased eosinophilic granules within interstitial cells. Less commonly, there were scattered inflammatory coagula in the interstitium that were sometimes centered on appreciable bacteria.

Morphologic Diagnosis: Varied, including: bacterial hepatopancreatitis, trematodiasis, and interstitial granule depletion.

Discussion:

American horseshoe crabs (HSC; *Limulus polyphemus*) are arthropods representing the only extant member of the genus *Limulus* (David R. Smith, 2017). They are living fossils and have persisted for more than 200 million years (Walls, Berkson, & Smith, 2002). HSC are marine invertebrates that migrate to deep ocean waters in the winter, and move to shallow waters to spawn in the summer. Sources of mortality in wild populations include complications of hemolymph collection for biopharmaceutical production, natural predation, commercial harvest for bait, spawning habitat loss, pollution, bycatch, climate change, and collection of specimens for research, education, and aquaria (David R. Smith, 2017). HSC are used heavily by the biopharmaceutical industry for an enzyme in their hemolymph called limulase amebocyte lysate (LAL), which detects small quantities of endotoxin. Due to this property, the Food and Drug Administration requires that nearly all pharmaceutical products are tested with LAL prior to market to screen for contamination (Elizabeth A. Walls, 2003; Rebecca L. Anderson, 2013).

The hepatopancreas is a large organ that occupies the majority of the prosoma (*i.e.* largest and most anterior body segment) of HSC. It fills the space around other organs in the prosoma and interdigitates with skeletal muscle of the legs and the reproductive tissue (*i.e.* either testes or ovaries in this dioecious species) (Bergdale, 2017). Additionally, hepatopancreas surrounds multiple hemocoel sinuses containing

hemocytes (*i.e.* the only immune cell of this species). The organ is composed mostly of interstitial cells interrupted regularly by large collecting tubules (Fahrenbach, 1999).

Collecting tubules branch from the anterior midgut and branch extensively thereafter. Tubules vary from 50-500 micron in diameter, have simple, tall, columnar epithelial cells with two primary cell types, and are surrounded by a 1-micron-thick basement membrane and a muscular network composed of circular and longitudinal striated muscle (Herman & Preus, 1972). A third cell type, enteroendocrine cells, are scattered basally, and are roughly spherical with abundant eosinophilic granules; similar cells are in the intestinal mucosa. The two primary cell types in the tubule epithelium are light cells (also called acidophils) and dark cells (also called basophils), named for their staining characteristics by light microscopy with HE staining. Dark cells are narrow at the base, wider near the lumen, and have secretory granules. Dark cells are analogous to the exocrine pancreas of mammals, and discharge enzymes such as lipase, amylase, and trypsin; as such, their granules may be referred to as “zymogen granules.” Light cells are much more numerous (approximately four times) than dark cells. These are phagocytic cells that ingest fine food particles, digest the particles, and presumably pass on the contents to interstitial cells (see below) (Fahrenbach, 1999). Pathologic changes to the collecting tubules were not a common feature in this series.

Interstitial cells (also referred to in some literature as “reserve cells”) are storage cells. They are large with vacuolation and abundant eosinophilic, spherical granules and fewer, smaller basophilic granules that vary in size and shape. Eosinophilic granules are typically abundant in interstitial cells of well-fed animals, and are especially abundant in the hepatopancreas around the heart, gut, and central nervous system (Herman & Preus, 1972). In starved HSC, interstitial cells have reduced cytoplasm that ultrastructurally lacks large protein granules, has reduced numbers of small protein granules, and lacks glycogen (Herman & Preus, 1972). In some cases in this series, the amount of eosinophilic granules within interstitial cells of the hepatopancreas was reduced. The significance of this finding is unclear. A possible cause is decreased overall nutritional status. Arthropods do not have grossly or histologically appreciable adipose stores, and as such, changes to the hepatopancreas are speculatively the most reflective organ of nutritional status. The amount of eosinophilic granules in interstitial cells appeared to vary somewhat in different regions of the hepatopancreas, which may complicate interpretation.

Metacercarial cysts are typically spherical with a double cyst wall. Some species with developing metacercariae in cysts have folded bodies within the cyst wall, the suckers of which are not readily evident in section (Laruelle, Molloy, & Roitman, 2002). This appears to be the morphology of the metacercariae in these HSC, which were tentatively identified as *Microphallus limulus*. *M. limulus* is a very common digenetic trematode that is reportedly present in “almost every” wild, 1-year-old HSC. The first intermediate host is a snail, within which the parasite transitions from a miracidium to a sporocyst to a cercariae. The cercariae exits the first intermediate host and invades juvenile HSC, encysting and forming metacercariae. Completion of the lifecycle occurs if HSC are consumed by birds. In HSC, metacercariae cysts of *M. limulus* form complex shells, which are approximately 200 micron, and filled with globular internal structure, as seen in this series. Encysted metacercariae of *M. limulus* are common in many types of connective tissue in HSC, and have also been reported in the eye and central nervous system. HSC that survive to adulthood frequently have degenerate cysts (Stunkard, 1951; Fahrenbach, 1999). *M. limulus* reportedly causes little host reaction, however, in the cases presented here, hemocytic response was occasionally seen, which may represent an early stage of infection.

Hemocytes are the only immune cell of HSC and are stored in vascular sinuses. Hemocytes were observed surrounding parasites and bacteria in the hepatopancreas in this series. Under normal physiologic conditions, hemocytes have granules in their cytoplasm. In pathologic conditions, hemocytes can discharge their cytoplasmic granules (*i.e.* become “agranular hemocytes”) and aggregate around wounds, infectious agents, and foreign material to aid in the immune response (Burse, 1977; Stagner & Redmond, 1974). Hemocyte granules contain a number of recognized antimicrobial substances, agglutinins, and factors to activate clotting. When clotting factors are released, this activates coagulation, and results in the formation of an insoluble coagulation gel, also called a coagulum. This coagulum occludes wounds and engulfs and immobilizes microbes, which are subsequently killed by antimicrobial substances released from hemocyte granules and entrapped in the coagulum (Muta & Iwanaga, 1996). A range of immune responses, including hemocytic infiltration and coagulation formation, were observed in this series.

References:

- Bergdale, K. J. (2017). *Illustrations for Health Assessment Techniques of the Atlantic Horseshoe Crab, Limulus polyphemus*. Thesis, Johns Hopkins University, Baltimore, MD.
- Burse, C. R. (1977). Histologic response to injury in the horseshoecrab, *Limulus polyphemus*. *Canadian Journal of Zoology*, 55, 1158-1165.
- David R. Smith, H. J.-R. (2017). Conservation status of the American horseshoe crab (*Limulus polyphemus*): a regional assessment. *Reviews in Fish Biology and Fishery*, 27(1):135-175.
- Elizabeth A. Walls, J. B. (2003). Effects of blood extraction on horseshoe crabs (*Limulus polyphemus*). *Fishery Bulletin*, 101: 457-459.
- Fahrenbach, W. H. (1999). Merostomata. In F. W. Harrison, & M. Locke (Eds.), *Microscopic Anatomy of Invertebrates* (Vol. 8A: Chelicerate Arthropoda, pp. 21-115). New York: Wiley-Interscience.
- Herman, W. S., & Preus, D. M. (1972). Ultrastructure of the hepatopancreas and associated tissues of the chelicerate arthropod, *Limulus polyphemus*. *Z. Zellforsch.*, 134(2), 255-271.
- Laruelle, F., Molloy, D. P., & Roitman, V. A. (2002). Histological analysis of trematodes in *Dreissena polymorpha*: their location, pathogenicity, and distinguishing morphological characteristics. *Journal of Parasitology*, 88(5), 856-863.
- Muta, T., & Iwanaga, S. (1996). Clotting and immune defense in Limulidae. *Progress in molecular and subcellular biology*, 15, 154-189.
- Rebecca L. Anderson, W. H. (2013). Sub-lethal behavior and physiological effects of the biomedical bleeding process on the American horseshoe crab, *Limulus polyphemus*. *Biology Bulletin*, 225(3): 137-151.
- Stagner, J. I., & Redmond, J. R. (1974). *The immunological mechanisms of the horseshoe crab, Limulus polyphemus*. Thesis, Iowa State University, Ames, Iowa.
- Stunkard, H. W. (1951). Observations on the morphology and life-history of *Microphallus limuli* n. sp. (Trematoda: Microphallidae). *Biological Bulletin*, 101(3), 307-318.
- Walls, E. A., Berkson, J., & Smith, S. A. (2002). The horseshoe crab, *Limulus polyphemus*: 200 million years of existence, 100 years of study. *Reviews in Fisheries Science*, 10(1), 39-73.

Disclaimer: The views expressed in this abstract are those of the author and do not reflect the official policy of the Army, Navy, Air Force, Department of Defense, or U.S. Government.

NEVPC Case 17

IDENTIFICATION NUMBER ON SOURCE MATERIAL: 4103795-00

SIGNALMENT: 19-year-old male Baboon (*Papio hamadryus*)

HISTORY: Apparently healthy, euthanized for colony management purposes.

GROSS FINDINGS: No significant findings

HISTOPATHOLOGIC FINDINGS: Pancreas: There are two proliferative lesions in the pancreas adjacent to a major pancreatic duct composed of small duct-like structures (i.e. ductular proliferation) admixed with individualized and, rarely, nests of polygonal cells supported on a fine fibrovascular stroma. The cytoplasmic and nuclear features are bland, including distinct cell borders, a moderate amount of pale eosinophilic cytoplasm, a single round to ovoid often basilar nucleus with finely stippled chromatin and generally one distinct nucleolus. Anisocytosis and anisokaryosis are minimal, and no mitoses are seen. Multifocally within several pancreatic islets there is a minimal amount of eosinophilic hyaline material; however, a Congo red stain (not submitted) fails to reveal any material with apple green birefringence.

Immunohistochemistry:

Pancytokeratin (AE1/AE3): Strong cytoplasmic immunoreactivity of duct-like epithelial cells (approximately 70-80% of cells within the proliferative foci).

CK19: Strong cytoplasmic immunoreactivity of duct-like epithelial cells (approximately 70-80% of cells within the proliferative foci)

Synaptophysin: Strong cytoplasmic immunoreactivity of individual and nest of polygonal cells (approximately 20-30% of cells within the proliferative foci)

Chromogranin: Strong cytoplasmic immunoreactivity of individual and nest of polygonal cells (approximately 20-30% of cells within the proliferative foci)

Insulin: Moderate cytoplasmic immunoreactivity of individual and nests of polygonal cells (approximately 30% of cells within the proliferative foci, indicative of beta islet cells)

Glucagon: Moderate cytoplasmic immunoreactivity of individual and nests of polygonal cells (approximately 2% of cells within the proliferative foci, indicative of alpha islet cells)

MORPHOLOGIC/ETIOLOGIC DIAGNOSIS: Pancreas: Nesidioblastosis, multifocal, moderate.

DISCUSSION:

Based on the cellular histomorphology of the proliferating cells and their immunohistochemical profiles (confirming both epithelial and neuroendocrine differentiation), these findings are consistent with a process that has been referred to as nesidioblastosis (“nesidio” refers to islet, and “blastosis” refers to proliferation). In this condition, islet neof ormation (including islet beta cells with variable proportions of other islet cells) proceeds from ductal epithelial cells with formation of ductal-acinar complexes. These may form focal to multifocal or diffuse hyperplastic lesions. Nesidioblastosis is occasionally reported in the human literature in association with hyperinsulinemic hypoglycemia, and has been suggested as a process for the physiologic as well as pathologic development of new islets. In veterinary medicine, this

condition is most commonly an incidental finding in normoglycemic animals, but has been reported in association with hyperglycemia in two squirrel monkeys.

Baboons are a well-characterized model of type II diabetes, including a predisposition toward islet amyloidosis. Insulin-resistant type II diabetes results in a compensatory islet beta cell proliferation as the body calls for more insulin, and because beta cells proliferate from dedifferentiated ductular tissue (and possibly from mitotic mature beta cells), it would logically follow that baboons may be predisposed to nesidioblastosis.

REFERENCES:

1. Fernandes A, King LC, Guz Y, Stein R, Wright CV, Teitelman G. Differentiation of new insulin-producing cells is induced by injury in adult pancreatic islets. *Endocrinology*. 1997;138:1750-1762.
2. Fujisawa H, Zhang Z, Sun W, Huang M, Kobayashi J, Yasuda H, Kinoshita Y, Ando R, Tamura K. Histopathological changes in the pancreas from a spontaneous hyperglycemic cynomolgus monkey. *J Toxicol Pathol*. 2012;25(215-219).
3. Furukoka H, Shirakawa T, Taniyama H, Ohishi H, Satoh H, Itakura C. Histogenesis of neoformation in the endocrine pancreas of aging horses. *Vet Pathol*. 1989;26(1):40-46.
4. Goossens A, Gepts W, Saudubray JM, Bonnefont JP, Nihoul-Fekete, Heitz PU, Kloppel G. Diffuse and focal nesidioblastosis. A clinicopathological study of 24 patients with persistent neonatal hyperinsulinemic hypoglycemia. *Am. Jour. Surg. Pathol*. 1989;13(9):766-775.
5. Guardado-Mendoza R, Davalli AM, Chavez AO, Hubbard GB, Dick EJ, Majluf-Cruz A, Tene-Perez CE, Goldschmidt L, Hart J, Perego C, Comuzzie AG, Tejero ME, Finzi G, Placidi C, La Rosa S, Capella C, Halff G, Gastaldelli A, DeFronzo RA, Folli F. Pancreatic islet amyloidosis, beta-cell apoptosis, and alpha-cell proliferation are determinants of islet remodeling in type-2 diabetic baboons. *Proc Natl Acad Sci USA*. 2009;106(33):13992-13997.
6. Hambrook LE, Ciavarella AA, Nimmo JS, Wayne J. Hyperinsulinaemic, hypoglycaemic syndrome due to acquired nesidioblastosis in a cat. *J Feline Med and Surg*. 2016;2(2):1-5.
7. Jubb KVF, Stent AW. Pancreas. In: Maxie MG, ed., *Jubb, Kennedy, and Palmer's Pathology of Domestic Animals*. Vol. 2. 6th ed., New York, NY: Elsevier Limited; 2016:353-375.
8. King CS, Streett JW, Moody KD, Barthold SW. Nesidioblastosis associated with hyperglycemia in two squirrel monkeys (*Saimiri sciureus*). *J Med Primatol* 1996;25:361-366.
9. Palladino AA, Stanley CA. Nesidioblastosis no longer! It's all about genetics. *J Clin Endocrinol Metab*. 2011;96(3):617-619.
10. Rumilla KM, Erickson LA, Service FJ, Vella A, Thompson GB, Grant CS, Lloyd RV. Hyperinsulinemic hypoglycemia with nesidioblastosis: histologic features and growth factor expression. *Modern Pathol*. 2009;22:239-245.
11. Service GJ, Thompson GB, Service FJ, Andrews JC, Collazo-Clavell ML, Lloyd RV. Hyperinsulinemic hypoglycemia with nesidioblastosis after gastric bypass surgery. *N Engl J Med*. 2005;353(3):249-254.
12. Solcia E, Capella C, Kloppel G. Tumors of the pancreas. In: *Atlas of tumor pathology*. 3rd series, Fascicle 20. Washington, D.C.: Armed Forces Institute of Pathology, 1997:120-44.

13. Son WC, Faki K, Mowat V, Gopinath C. Spontaneously occurring extra-islet endocrine cell proliferation in the pancreas of young Beagle dogs. *J Toxicology Letters*. 2010;193:179-182.

NEVPC Case 18

CONTRIBUTOR(S)/INSTITUTION: L. Clayton Apgar, University of Pennsylvania

SIGNALMENT: 12 year old male castrated Australian shepherd dog

HISTORY:

The patient was euthanized following diagnosis of hemopericardium and suspect right atrial hemangiosarcoma. Four months prior to euthanasia, the dog was presented with hemoabdomen and a ruptured splenic mass diagnosed as hemangiosarcoma following splenectomy. He was enrolled in a clinical trial to evaluate the safety and effectiveness of a gene therapy protocol using an anti-vascular endothelial growth factor (VEGF) vector. Beginning approximately two weeks after diagnosis, the dog received a total of 5 doses of doxorubicin chemotherapy, and either placebo or anti-VEGF vector treatment, and regular monitoring for evidence of progression of disease. Treatments were tolerated well and the patient showed no signs of progression until presenting to the emergency service. Given the grave prognosis once pericardial effusion was identified, humane euthanasia was elected. The dog had no radiographic evidence of metastasis at a recheck visit one month prior to euthanasia.

GROSS FINDINGS:

Relevant gross findings included 20 mL of hemorrhagic fluid within the pericardial sac. The epicardial surface of the right auricle contained multiple pinpoint to 0.3 cm diameter soft, minimally bulging, dark red, blood-filled nodules. Expanding the endocardial surface of the right auricle and occupying approximately 80% of the auricular chamber was a 2.5 x 1.2 x 2.0 cm red-pink, firm, bilobed nodule with a central blood-filled cavity.

Cranial lung lobes bilaterally contained innumerable pinpoint to 0.3cm diameter multifocal to coalescing, hard, white nodules elevating the pleura and extending into the parenchyma, and a single fibrous adhesion from the left cranial lung lobe to the parietal pleura. The middle and caudal lung lobes were grossly unremarkable, and sections from the affected and grossly normal lungs floated in 10% formalin. The remainder of gross findings were unremarkable.

HISTOPATHOLOGIC/CYTOLOGIC FINDINGS:

Submitted slides include sections from the grossly affected cranial lobes and grossly normal caudal lobes from the right and left sides, respectively. Throughout the affected lobes, there were numerous, up to 0.3cm diameter, round to irregular foci of lamellar bone with alveoli and occasionally within the interstitium. There were few smaller irregular foci of non-bone mineralization. The adjacent interstitium was expanded by mild to moderate amounts of fibrous connective tissue, small amounts of predominantly lymphoplasmacytic and histiocytic infiltrate, and few multinucleated giant cells, and mild congestion. On histologic examination, grossly unaffected lung contained minimal multifocal pulmonary edema with alveolar histiocytosis.

The right atrial mass was confirmed as hemangiosarcoma. Other relevant findings included marked multifocal endocardial and epicardial fibrosis and hemorrhage, moderate chronic-active lymphoplasmacytic and neutrophilic epicarditis and endocarditis in the right ventricle and atrium. The left ventricular free wall and interventricular septum contained mild acute to subacute multifocal myocardial necrosis and interstitial fibrosis. There was mild hepatic centrilobular congestion in all sections of liver examined.

Histopathologic examination of the kidneys revealed bilateral, mild segmental glomerulopathy characterized by glomerular basement membrane thickening without hypercellularity, and rare glomerulosclerosis, along with mild to moderate multifocal chronic lymphoplasmacytic tubulointerstitial nephritis.

The remainder of histopathologic findings were unremarkable.

MORPHOLOGIC/ETIOLOGIC DIAGNOSIS:

1. Dog, cranial lung lobes, marked multifocal pulmonary alveolar microlithiasis with ossification with moderate interstitial fibrosis and rare lymphoplasmacytic and histiocytic infiltrates
2. Dog, right atrium, hemangiosarcoma
3. Dog, left ventricular free wall and interventricular septum, multifocal myocardial necrosis and fibrosis
4. Dog, kidneys, mild multifocal segmental glomerulopathy with rare glomerulosclerosis and mild to moderate multifocal lymphoplasmacytic tubulointerstitial nephritis

DISCUSSION:

The most striking feature on gross and histopathologic examination was the pulmonary alveolar microlithiasis and ossification. Similar histologic findings in a dog have been reported, one in which the dog presented with a history of shortness of breath¹, and in a dog with multicentric mammary tumors⁵. The latter case also possessed pulmonary metastases of mammary tumors, left ventricular hypertrophy, and right ventricular dilation. No evidence of hemangiosarcoma within the lungs was identified in the present case.

Despite histologic findings of myocardial necrosis and fibrosis, the dog was reportedly acting normally and tolerating therapy well until presentation with acute pericardial effusion. The lesions seen in the left ventricular free wall and interventricular septum are considered as a possible case of doxorubicin toxicity⁴. Some reports of pulmonary ossification in the human literature are considered secondary to right heart failure³, which is considered a possible factor in this patient, given the presence of right atrial hemangiosarcoma and centrilobular hepatic congestion, though clinical data supporting heart failure are not available.

Proposed theories for the pathogenesis of alveolar microlithiasis include inflammation or inappropriate immune response leading to exudate within alveoli, which then acts as a nidus for the formation of microliths. Other theories include exposure to inhaled irritants, or errors of metabolism leading to decreased solubility of calcium phosphate in an alkaline environment¹. While this alveolar microlithiasis is considered idiopathic, other possible causes of pulmonary calcification, mostly interstitial, are considered the result of metastatic or dystrophic processes² for which we have no supporting evidence in the present case. This is presented as a curious case of rapidly forming and prolific alveolar microlithiasis and ossification in a dog with hemangiosarcoma and evidence of possible cardiac insufficiency.

REFERENCES:

1. Brix, A. E., et al. "Pulmonary Alveolar Microlithiasis and Ossification in a Dog." *Veterinary Pathology*, vol. 31, no. 3, 1994, pp. 382-385., doi:10.1177/030098589403100314.
2. Chan, Edward D., et al. "Calcium Deposition with or without Bone Formation in the Lung." *American Journal of Respiratory and Critical Care Medicine*, vol. 165, no. 12, 2002, pp. 1654-1669., doi:10.1164/rccm.2108054.
3. Jamjoom L, Meziane M, Renapurkar RD. "Dendriiform pulmonary ossification: Report of two cases." *The Indian Journal of Radiology & Imaging*. 2013;23(1):15-18. doi:10.4103/0971-3026.113613.
4. Mauldin, Glenna E., et al. "Doxorubicin-Induced Cardiotoxicosis Clinical Features in 32 Dogs." *Journal of Veterinary Internal Medicine*, vol. 6, no. 2, 1992, pp. 82-88., doi:10.1111/j.1939-
5. Kubba, Mahir A.g. "Pulmonary Ossification and Microlithiasis in a Bitch with Multicentric Mammary Tumors." *Open Veterinary Journal*, vol. 7, no. 3, 2017, p. 273., doi:10.4314/ovj.v7i3.12.

ACKNOWLEDGMENTS:

Thank you to Dr. Molly Church and Dr. Julie Engiles of the University of Pennsylvania for your help with this case.

NC STATE UNIVERSITY

1060 William Moore Drive
Raleigh, NC 27607

NEVPC Case 19
Slide #: 17-2362-1

919.513.6240 (Department Head)
Administrative Office)
919.513.6464 (Fax)

Contributors: Megan E. Schreeg, Debra A. Tokarz
Institution: North Carolina State University

Signalment: 10 year old female spayed domestic longhair cat

History: The cat presented to North Carolina State University Veterinary Teaching Hospital for further evaluation of renal sarcoma, which was diagnosed by fine needle aspirate (FNA) after renomegaly was incidentally identified on abdominal radiographs by the referring veterinarian. Abdominal ultrasound revealed bilateral renal masses, and FNA of the second renal mass was consistent with sarcoma with necrosis. Serum biochemistry panel revealed a normal BUN and creatinine, and urine specific gravity was 1.038. Symmetric dimethylarginine (SDMA) was elevated at 21 ug/dl (RR 0-14 ug/dl). The cat was initially asymptomatic, and thus was managed conservatively at home until clinical decline and euthanasia approximately 3 weeks after initial presentation.

Gross findings: Heart: Transmurally expanding the cardiac musculature at the apical left ventricle was a focal 1x 2 x 3 cm white firm plaque-like mass. Scattered throughout this mass were multifocal to coalescing petechiae. Similar 2-3 mm white foci were present throughout the interventricular septum and left ventricular free wall. Lung: Scattered throughout all lung lobes were approximately 20 pinpoint to 3 mm, white to tan, firm, nodules that extended into the lung parenchyma on cut surface. Kidneys: Bilaterally the caudal poles of the kidneys were expanded by firm, raised, masses that were well adhered to overlying capsule. On sagittal section, the caudal 1/2 of the right kidney and caudal 1/3 of the left kidney were completely effaced by firm, white, poorly demarcated masses with scattered softer foci. Within the right renal mass, at the site of the corticomedullary junction there was a sharp white line surrounded by gelatinous, yellow-brown tissue. Approximately 5-10, similar, 2-6 mm diameter round masses were scattered through the remainder of the right kidney. Multifocally in both kidneys were bright red, wedge-shaped well-demarcated foci that extended from cortex to medulla.

Histopathology: Heart: Dissecting between and effacing approximately 40% of the normal myocardium in the examined section is an infiltrative, poorly demarcated, unencapsulated, moderately cellular neoplasm that is composed of bundles, streams, and whorls of pleomorphic spindle-shaped cells that are embedded in a minimal fibrovascular matrix. The majority of neoplastic cells are spindloid and markedly elongated, but occasionally are round. Cell borders are variably distinct, and cells have scant to moderate amphophilic cytoplasm and round to elongated centrally located nuclei with finely stippled chromatin and 1-2 prominent nucleoli. There is marked anisocytosis and anisokaryosis, with 6 mitotic figures per 10 HPF. Bizarre mitotic figures are prominent, and there are frequent multi-nucleated cells, including multi-nucleated giant cells, throughout the neoplasm. A mixed population of inflammatory cells (neutrophils, lymphocytes, macrophages) is intermixed with neoplastic cells and intact to necrotic cardiac myofibers. There are multifocal lakes of lytic necrosis throughout the neoplasm, characterized by loss of cellular features and accumulation of pale, eosinophilic material and cellular debris intermixed with degenerative inflammatory cells and multi-focal hemorrhage. A large caliber vessel present within the affected myocardium is occluded by neoplastic cells (vascular neoplastic embolism).

Similar neoplastic cells are identified in both kidneys, including within multiple vessels, and are associated with marked lytic necrosis. Neoplastic cells are also identified in lungs as well as splenic vessels.

Immunohistochemistry: Immunohistochemical stains for myoglobin, smooth muscle actin, muscle-specific actin, and Factor VIII as well as PTAH stain are applied to cardiac tissue. Neoplastic cells are positive for smooth muscle actin and muscle-specific actin, and negative for myoglobin and Factor VIII. Cross striations are not identified in neoplastic cells with PTAH stain.

Morphologic Diagnosis: Heart, kidneys (bilateral), lungs, splenic vessels: Cardiac leiomyosarcoma with multifocal metastasis and neoplastic thromboembolism with acute renal infarction and ischemic necrosis

NC STATE UNIVERSITY

Discussion: Based on the pattern of organ involvement, gross and histologic examination, and immunohistochemistry, this case is consistent with a primary cardiac leiomyosarcoma with hematogenous metastasis to the kidneys and lungs. To our knowledge, this is the first report of a primary cardiac leiomyosarcoma in a feline patient.

1060 William Moore Drive
Raleigh, NC 27607
919.513.6240 (Department Head
Administrative Office)
919.513.6464 (Fax)

Cardiac neoplasms, including both primary and secondary, are rarely reported in the literature in cats. Metastatic neoplasia of the heart, including various carcinomas and lymphomas, have been most commonly reported. Primary neoplasms reported in cats include single case reports of a rhabdomyosarcoma, hemangiosarcoma, and an undifferentiated sarcoma.

Leiomyosarcoma arising from the pulmonary artery has been reported in one dog. Leiomyosarcoma arising from the great vessels and the heart itself (the latter referred to as primary cardiac leiomyosarcoma, or PCLMS) has been reported more extensively in the human literature, but is still considered a rare neoplasm. In a review of PCLMS in humans (n=79), over half of the neoplasms arose from left atrium, while only 5.1% arose from the left ventricle, as in the current case. The vast majority of patients in this study presented with respiratory (e.g. dyspnea) or cardiac (e.g. tachycardia) symptoms, although rarely, patients were asymptomatic, as with this case. Metastatic disease was reported in 32 cases, and overall, patients with cardiac leiomyosarcoma had a poorer prognosis and survival rate than patients with leiomyosarcomas arising from other locations (e.g. uterus).

In this case, the primary neoplasm is thought to have arisen from the smooth muscle of a vessel within the left ventricular wall. Therefore, a mixed vascular/smooth muscle tumor (angioleiomyosarcoma) was also considered, a neoplasm which has been reported arising in the esophagus of a cat. However, this was ruled out with negative Factor VIII staining of neoplastic cells.

This patient originally presented for evaluation of suspected sarcoma of the kidney, and was eventually found to have bilateral renal masses cytologically consistent with sarcoma. Renal neoplasia is relatively rare in cats. Lymphoma and renal cell carcinoma are the most commonly reported primary renal neoplasms, with sarcomas being only rarely reported, including one recent report of a renal leiomyosarcoma. Therefore, detection of bilateral sarcoma in the kidneys of a cat should be suspected to represent metastatic disease and should prompt systemic staging to look for a primary neoplastic source. Interestingly, in this case extensive staging was performed, including echocardiography, but the cardiac mass was not detected, likely due to the infiltrative nature of neoplasm as well as patient body habitus that precluded optimal imaging.

Last, it is interesting to note that this patient was not azotemic on initial presentation, but did have an elevated SDMA, which correlated well to the percentage of renal parenchyma (approximately 60-70%) affected by neoplasia and infarction. This finding supports the use of SDMA as an earlier biomarker of loss of renal function.

References

1. Aupperle, et al. Primary and secondary heart tumours in dogs and cats. *J Comp. Path* 2007, 136:18-26.
2. Baker and Goodwin. Pulmonary artery sarcomes: A review and report of a case. *Arch Path Lab Med* 1985, 109 (1): 35-39.
3. Callanan, et al. Primary pulmonary artery leiomyosarcoma in an adult dog. *Vet Path* 2000, 37: 663-666.
4. Evans and Fowlkes. Renal leiomyosarcoma in a cat. *J Vet Diag Inv* 2016, 28(3): 315-318.
5. Henry, et al. Primary renal tumours in cats: 19 cases (1992-1998). *JFMS* 1999, 1: 165-170.
6. Merlo, et al. Primary right atrium hemangiosarcoma in a cat. *JFMS* 2000, 4: 61-64.
7. Pessier, et al. Primary sarcoma of the heart in a cat. *Feline Practice* 1990, 18 (30): 25-27
8. Teo, et al. Oesophageal angioleiomyosarcoma in a cat. *JFMS* 2014, 16 (10): 846-852.
9. Venco, et al. Primary cardiac rhabdomyosarcoma in a cat. *JAAHA* 2001, 37: 159-163.
10. Wang, et al. Primary cardiac leiomyosarcoma: An analysis of clinical characteristics and outcome patterns. *Asian Cardiovascular and Thoracic Annals* 2015, 23 (5): 623-630.

Acknowledgments: We would like to thank Keith Linder, Brolin Evans, Julie Allen, Maria Evola, as well as Joanna Barton and the NCSU Histology Laboratory

1060 William Moore Drive
Raleigh, NC 27607

919.513.6240 (Department Head
Administrative Office)
919.513.6464 (Fax)

Slide #: 18-355

919.513.6240 (Department Head)
Administrative Office)
919.513.6464 (Fax)

Contributors: Amy Flis, Brigid Troan, Keith E. Linder
Institution: North Carolina State University

Signalment: 15 year old male castrated Domestic Longhair cat (*Felis catus*)

History: The cat first presented to the primary veterinarian in 2016 for a small, non-pigmented mass originating from the left nares. Histopathology at that time showed severe lymphoplasmacytic and eosinophilic nodular rhinitis and dermatitis. The mass inside the nares resolved, but the cat developed a large mass on the nasal planum. The cat was managed on Depo-Medrol with no clinical change. In November of 2017, the cat began losing weight with no cause identified. Due to severe, ongoing weight loss and more recent clinical dyspnea and dehydration, and the cat was euthanized in February. A full autopsy was not performed, but the nasal planum mass was submitted for histopathologic evaluation.

Gross findings: An 18 x 14 x 10 mm haired, non-ulcerated, skin mass was submitted in 10% buffered formalin.

Histopathology:

Haired skin: The dermis and superficial subcutis are markedly expanded by large, multifocal to coalescing regions of marked lytic necrosis surrounded by a thin rim of macrophages and hypertrophied and vacuolated stromal cells. The necrotic regions have low cellularity, abundant eosinophilic fluid, and a small amount of admixed cellular and karyorrhectic debris. Necrotic area margins have swollen, degenerating cells that often contain enlarged, vesiculate nuclei with peripheralized chromatin and pale amphophilic to eosinophilic inclusion bodies. Pyknotic and fragmented cells are intermixed. Near areas of necrosis, a few scattered small caliber vessels have fibrin, fragmented erythrocytes, and a few neutrophils and/or lymphocytes in and around the tunica media; occasionally thrombosis is observed. Widely surrounding necrotic foci, numerous aggregates of plasma cells and lymphocytes, scattered macrophages, and a few eosinophils are present in a perivascular to interstitial pattern. Adnexa are not involved, and the epidermis is intact. The unaffected dermis and subcutis frequently contain robust collagenous stroma.

Morphologic Diagnosis:

Haired skin: Marked, multifocal to coalescing, dermal necrosis with moderate, chronic, lymphoplasmacytic and mild eosinophilic cellulitis and vasculitis

Discussion: Histopathologic evaluation in this case revealed marked necrosis with inflammation that was predominantly histiocytic and lymphoplasmacytic with a lesser, but diagnostically significant, eosinophilic component. Intranuclear inclusion bodies in stroma cells and lytic necrosis led to a presumptive diagnosis of feline herpesvirus-1 (FHV-1) necrotizing dermatitis, which is an atypical presentation. Another deep infection or possibly feline eosinophilic granuloma complex were possible but unlikely differentials. Similarly, the reaction pattern and location were somewhat suggestive of mosquito bite hypersensitivity, but the presence of a large mass and lack of erosions, ulcers, crusts, and alopecia are not typical. Fixed-tissue immunohistochemical testing for FHV-1 revealed numerous immunoreactive cells along the periphery of the regions of lytic necrosis, which contained intranuclear inclusion bodies. Immunohistochemical results support FHV-1 as the cause for lytic dermal necrosis and vasculitis in this case, and this case may represent a novel presentation of FHV-1 induced disease.

Feline herpesvirus-1 is an alphaherpesvirus, a double-stranded DNA virus that infects domestic and wild felids. Infection induces cytolytic infections of typically mucosal epithelial cells and can establish latent infections in the trigeminal ganglion, optic nerve, olfactory bulb, and cornea. The virus is transmitted by contact with infected nasal or ocular secretions or by aerosol. Transmission by fomites is rare since the virus is short-lived in most environmental conditions. Viral replication in most cases occurs in the nasal mucosa, nasopharynx, sinuses, and tonsils, corresponding with the virus's optimal replication occurring at lower temperatures. Viremia is uncommon except in young kittens. Morbidity is high, but mortality is low with most cats recovering in 10-14 days and many cats becoming latently infected. Reactivation of latent infections may be induced by environmental stressors or corticosteroid therapy, which may have contributed to persistence of the lesion in this case. Up to 20-40% of recovered cats are expected to shed virus during times of stress. Clinical signs in infected cats include fever, oculonasal discharge, sneezing, coughing, and anorexia. Infection is widespread in most cat populations, but clinical signs are most common in kittens although adult cats can have recurrent clinical signs, presumably due to reactivation of latent infections. In clinical cases, gross lesions are typically restricted to sites of predilection for viral replication and include the epithelium of nasal passages, pharynx, soft palate, conjunctivae, tonsils, and trachea. Deeper infection of the lung is uncommon. In contrast to infection with feline calicivirus, ulceration of the tongue, hard palate, or nostrils is uncommon but does occur. Lesions of the skin are most often ulcerative lesions of haired skin of the face and nasal planum with rare reports of lesions on the feet and trunk. The classic microscopic finding of large pale amphiphilic and/or eosinophilic intranuclear inclusion bodies is transient and typically only present during the period of active viral replication 2-7 days post-infection of the respiratory tract. These inclusions may also be found in patients dying from disease but otherwise are rarely identified beyond 7 days. The timing of inclusion bodies in skin lesions may be different. Pulmonary involvement is not common except in fatal cases. Necrosis of pulmonary vessels with viral antigen in the vessel wall is rarely described. Systemic disease of FHV-1 is rare.

Chronic sequelae of FHV-1 infection include chronic rhinitis and sinusitis, and ocular lesions can also progress to chronic ulcerative keratitis. A less common disease pattern in cats, which may be associated with corticosteroid therapy in some cases, is the syndrome of ulcerative facial and nasal dermatitis and stomatitis that includes eosinophilic inflammation and low numbers of intranuclear inclusion bodies. Skin adnexa are often affected. This syndrome has been described in several case series in cats with a similar syndrome reported in cheetahs. This syndrome can be misdiagnosed as eosinophilic granuloma complex given the low numbers of viral inclusion bodies. FHV-1 has also been implicated in cases of chronic conjunctivitis and periocular skin disease in adult cats. In the presented case, although there is no characteristic ulceration in the examined tissue, the presence of intranuclear inclusion bodies and positive immunohistochemical staining support the diagnosis of FHV-1. PCR and fluorescent in situ hybridization may also be pursued to provide further evidence of FHV-1 as the causative agent.

1060 William Moore Drive
Raleigh, NC 27607

919.513.6240 (Department Head
Administrative Office)
919.513.6464 (Fax)

References

1. Caswell JL, Williams KJ. Respiratory system. In *Jubb, Kennedy, & Palmer's Pathology of Domestic animals*. 6th ed. St. Louis, MO: Elsevier; 2016.
2. Gaskell R, Dawson S, Radford A, Thiry Etienne. Feline herpesvirus. *Vet Res*, 2007. 38: 337-354.
3. Hargis AM, Ginn PE. Feline herpesvirus 1-associated facial and nasal dermatitis and stomatitis in domestic cats. *Vet. Clin. North Am. Small Anim. Pract.* 1999; 29:1281– 1290.
4. Mauldin EA, Peters-Kennedy J. Integumentary System. In *Jubb, Kennedy, & Palmer's Pathology of Domestic animals*. 6th ed. St. Louis, MO: Elsevier; 2016.
5. Sánchez MD, Goldschmidt MH, & Mauldin EA. Herpesvirus dermatitis in two cats without facial lesions. *Veterinary dermatology*, 2012; 23(2), 171.
6. Suchy A, Bauder B, et al. Diagnosis of feline herpesvirus infection by immunohistochemistry, polymerase chain reaction and in situ hybridization. *J Vet Diagn Invest*, 2000; 12: 186-191.

Acknowledgments: Dr. Luke Borst and Ms Joanna Barton and the NCSU Histology Laboratory